Investigating Oligodendrocyte Myelin Glycoprotein as a Novel Autoantibody in Demyelinating Disorders with Atypical Features

by

Ceyda Nur Altınışık

A Dissertation Submitted to the
Graduate School of Health Sciences
in Partial Fulfillment of the Requirements for
the Degree of

Master of Science

in

Neuroscience

July 23, 2024

Investigating Oligodendrocyte Myelin Glycoprotein as a Novel Autoantibody in Demyelinating Disorders with Atypical Features

Koç University

Graduate School of Health Sciences

This is to certify that I have examined this copy of a master's thesis by

Ceyda Nur Altınışık

and have found that it is complete and satisfactory in all respects,
and that any and all revisions required by the final
examining committee have been made.

Committee Members:

Assoc. Prof Atay VURAL (Advisor)

Prof. Murat KURTUNCU

Assoc. Prof. Hale YAPICI ESER

Date: 23.07.2024

To M. Kemal ATATURK, my dearest family, and everyone who believes in the guidance of science!

ABSTRACT

Investigating Oligodendrocyte Myelin Glycoprotein as a Novel Autoantibody in Demyelinating Disorders with Atypical Features

Ceyda Nur Altınışık

Master of Science in Neuroscience

July 23, 2024

Over the past decade, boosting studies of autoantibodies associated with inflammatory disorders of the central nervous system (CNS) have further expanded the spectrum of demyelinating diseases. Especially, the discovery of anti-AQP4 and anti-MOG antibodies has enabled differential diagnostic criteria formation for patients with Neuromyelitis Optica Spectrum Diseases or MOG Antibody Disease, which are in the demyelinating disease group. Despite this, most patients in this spectrum are still either undiagnosed or misdiagnosed due to their atypical features, and the actual target of autoimmune responses is unknown. Associating relevant patients with novel autoantibodies to be discovered is crucial, particularly in making the proper treatment decisions and showing improvement. Oligodendrocyte myelin glycoprotein (OMGp) is a promising autoantibody candidate because it is a glycoprotein explicitly expressed on the surfaces of CNS neurons and oligodendrocytes. Therefore, this thesis aims to test anti-OMGp antibodies in a large and atypical feature-rich demyelinating disease cohort and to describe the clinical and radiological characteristics of anti-OMGp antibody-associated disease.

In this study, the “live cell-based assay”, a “gold standard” for numerous autoantibody detections, was first optimized and developed to detect anti-OMGp antibodies. Subsequently, the serum of 834 people, aged between 8 and 90, with a gender distribution of x:y, male: female, and the CSF of 86 patients were screened for anti-OMGp antibody positivity employing this test. The cut-off value was determined using 30 healthy controls. While net positivity was detected in seventeen sera, all CSF samples were negative. All patients with positive anti-OMGp antibodies had negative anti-MOG and anti-AQP4 antibodies; none had a typical MS diagnosis. The average age of positive cases is A (range 17-59), male-female ratio is B. Eight of the patients were diagnosed with atypical demyelinating disease, and one was diagnosed with autoimmune encephalitis. Atypical demyelinating features were as follows: tumefactive lesion in four patients, diffuse ADEM-like lesions in three patients, long segment transverse myelitis in two patients, and cortical lesion in one patient. The oligoclonal band was positive in 2/6 patients.

Thus, this study tested anti-OMGp antibodies in an atypical feature-rich demyelinating disease cohort for the first time in the literature; seventeen positive patients were identified. Atypical demyelinating disease features were detected in all positive patients regarding clinical, radiological, and treatment response. Our findings indicate that anti-OMGp antibodies may cause a distinct disease entity and should be tested, especially in individuals with atypical demyelinating disease characteristics.

ÖZETÇE

Atipik Özelliklere Sahip Demiyelinizan Bozukluklarda Yeni Bir Otoantikor Olarak Oligodendrosit Miyelin Glikoproteinin Araştırılması

Ceyda Nur Altınışık

Nörobilim, Yüksek Lisans

23 Temmuz 2024

Son on yılda, merkezi sinir sisteminin (MSS) inflamatuar bozukluklarıyla ilişkili antikorlara ilişkin artan çalışmalar, demiyelinizan hastalık spektrumunu daha da genişletmiştir. Özellikle anti-AQP4 ve anti-MOG antikorlarının keşfi demiyelinizan hastalık grubunda yer alan Nöromiyelitis Optika Spektrum Hastalıklar (NMOSD) veya MOG Antikor Hastalığ (MOGAD) hastaları için ayırıcı tanı kriterlerinin oluşmasını sağlamıştır. Buna rağmen, halen bu spektrumdaki hastaların çoğu atipik özellikleri sebebiyle ya tanı alamamakta ya da yanlış tanılar konulmakta ve otoimmün yanıtlarının gerçek hedefi bilinmemektedir. İlgili hastaların keşfedilecek yeni otoantikorlar ile ilişkilendirilmesi özellikle tedaviye ilişkin doğru kararlar alınması ve iyileşme gösterebilmeleri açısından oldukça önemlidir.Oligodendrosit miyelin glikoproteini (OMGp), özellikle MSS nöron ve oligodendrosit hücrelerinin yüzeylerinde eksprese edilen bir glikoprotein olduğu için iyi bir otoantikor adayıdır. Dolayısıyla bu tez çalışmasının amacı geniş ve atipik özellik bakımından zengin bir demiyelinizan hastalık kohortunda anti-OMGp antikorlarını test ederek; anti-OMGp antikoru ilişkili hastalığın klinik ve radyolojik özelliklerini tanımlamaktır.

Anti-OMGp antikorlarını tespit edebilmek için öncelikle, birçok otoantikor tespiti için "altın standart" olan "canlı hücre temelli test", optimize edilerek, geliştrilmiştir. Takiben, yaşları 8 ile 90 arasında değişen, cinsiyet dağılım oranı x:y, kadın: erkek olmak üzere toplam 834 kişinin serumu ve içlerinden 86 hastanın BOS'u anti-OMGp antikor pozitifliği açısından geliştirilen bu test aracılığıyla taranmıştır. 30 sağlıklı kontrol kullanılarak test sınır değeri belirlenmiştir. Serumların on-yedisinde net pozitiflik saptanırken, BOS örneklerinin hepsi negatif saptanmıştır. Anti-OMGp antikoru pozitif bulunan hastaların tümünde anti-MOG ve anti-AQP4 antikorları negatiftir ve hiçbiri tipik MS tanısı almamıştır. Pozitif olguların ortalama yaşı A (dağılım C), kadın-erkek oranı B idir. Sekiz hasta atipik demiyelinizan hastalık, bir hasta ise otoimmün ensefalit tanısına sahipti. Atipik demiyelinizan özellikler: dört hastada tümefaktif lezyon, üç hastada ADEM-benzeri yaygın lezyonlar, iki hastada uzun segment transvers miyelit, bir hastada kortikal lezyon şeklindeyken altı hastanın ikisinde pozitif oligoklonal bant mevcuttu.

Bu çalışma ile literatürde ilk kez atipik özellikler bakımından zengin bir kohortta anti-OMGp antikorları test edilerek onyedi pozitif hasta tanımlanmıştır. Her pozitif hastada radyolojik, klinik, ve tedaviye yanıt açılarından atipik demiyelinizan hastalık özellikleri bulunmuştur.. Bulgularımız anti-OMGp antikorlarının ayrı bir hastalık antitesine yol açabileceğini ve özellikle atipik demiyelinizan hastalık özelliği gösteren kişilerde anti-OMGp antikorlarının test edilmesi gerektiğini göstermektedir.

ACKNOWLEDGEMENTS

Firstly, I would like to thank my dear advisor, Assoc. Prof. Atay Vural. It has been exceptional and invaluable that he believed in me more than I do, helped me discover my potential in every sense, and supported me under all circumstances with his passion for teaching. I am deeply grateful to him, who provided me the return chance to my education life, which I had to freeze for various reasons, and for welcoming me with the same warmness, mentorship, and dedication upon my return. I learned a lot from him, theoretically and academically, and I could not have done it without his guidance; I thank him for everything he has given me with his unique perspective.

I would like to thank my thesis committee, Prof Murat Kurtuncu, and Assoc. Prof. Hale Yapıcı Eser for accepting to be my jury member.

I would like to express my endless gratitude to Prof. Tamer Önder, to whom I owe a heartfelt thankfulness for the light he shed on my path during the most challenging period of my life and for making this day possible. With his guidance, my journey here allowed me to grow practically, scientifically, and academically. The fact that I can perform rapid troubleshooting in the laboratory today is undoubtedly thanks to the scientific thinking ability I gained from him. I will carry the pride of being able to learn numerous new molecular techniques from him throughout my life, and I will never forget his paternal attitude and support during the difficulties I experienced.

I would also like to thank KUTTAM's Flow Cytometry "virtuoso," dear Dr. Özgür Albayrak, for training me tremendously in this technique, even though I knew nothing about Flow, and for patiently listening to and answering every scientific question I asked. Whenever I felt lost in my academic journey, the person who pulled me out was Dr. Özgecan Kayalar. Our scientific discussions with you two were delightful; thank you both!

I met wonderful people during my duration at KUTTAM. While I would like to thank every colleague with whom I have created great memories, I would like to underline a few names. My lovely friends with whom I shared my first and most memorable moments here: Arda, Canan, Ebru, and Gizem Söyler; my friends from Vural Lab team who warm-welcomed me with their aids: Hussein, Nazan, Kardelen, Ergün, Kaan, Mine, Mina and Mohammad Reza; my first friends at KUH ; Ecem, Gizem, Sema and my precious friend

Merve in who friendship started with our undergraduate path, reached the top with Erasmus memories and was strengthened here.

The thesis process was bearable, thanks to my buddies with whom I laughed and cried together. I would like to thank each of them individually; however, I would especially like to mention my best friends: Büşra, Nurçin, and Fatmanur. I appreciate you guys for never letting my mood drop, being my motivation to continue this road by adding energy to my energy, and being there at the moment, without question, whenever I need it. Your friendship is priceless; I am glad to have all of you in my life. Fikret Feyza, my flatmate, who has specially placed my heart in a short time, the conversations we have with you, our yoga sessions, the podcasts we recommend to each other, and the many things we experience and discover together have a completely charming taste. Thank you for being in my life, gorgeous sis!

The most special thanks belong to my only family. My dear mother, Hatice, and my father, Mevlüt, they are my two most irreplaceable miracles. I am indebted with genuine appreciation to their work, regardless of day or night, for their children's education by constructing opportunities from impossibilities. With their sacrifices and faith in me, my education became my incalculable golden bracelet. I know my adorable sister, Sümeyra, and my brothers, Yunus and Emre, are prouder of my achievements than I am. I cannot thank them enough for caring and supporting me under all circumstances throughout my education.

Finally, I want to leave as a note for the future: Dear Cey, I am proud of you for not giving up and continuing to strive despite all the difficulties you have experienced in life. Keep going because you are blossoming!

TABLE OF CONTENTS

List of Tables xi

List of Figures xii

List of Supplementary Figures xiii

Abbreviations xiv

Chapter 1: Introduction 1

1.1 Overview 1

1.2 Aim & Hypothesis 3

Chapter 2: Literature Review 4

2.1 Introductory Concepts: Myelination, Demyelination, and Remyelination 4

2.2 Demyelinating Diseases 5

2.3 Demyelinating Disease Types of the CNS 7

2.3.1 Multiple sclerosis (MS) 7

2.3.2 Neuromyelitis optica spectrum disorder (NMOSD) 10

2.3.3 Myelin oligodendrocyte glycoprotein antibody-associated disease (MOGAD) 13

2.3.4 Optic Neuritis (ON) 15

2.3.5 Transverse myelitis (TM) 17

2.3.6 Acute disseminated encephalomyelitis (ADEM) 19

2.4 Oligodendrocyte myelin glycoprotein (OMGp) 21

2.4.1 Struction 22

2.4.2 Localization 25

2.4.3 Function 26

2.5 Live Cell Based Assay to Detection of Autoantibodies 29

2.6 Autoantibodies Against anti-OMGp 31

Chapter 3: method 31

3.1 Plasmid Obtaining 31
3.1.1 pOMGP-TM-GFP & pEGFP-N1 plasmid Elution 31
3.1.2 Bacterial Growth Medium Preparation 32
3.1.3 Competent Bacteria Preparation 32
3.1.4 Bacterial Transformation 33
3.1.5 Plasmid DNA Purification and Diagnostic Digestions 34
3.2 Cell Culture 35
3.2.1 HEK293 and HeLa Cell Culture 35
3.2.2 Transfection Optimizations 35
3.3 Optimization of Live Cell Based Assay 36
3.3.1 Culturing and Transfection of Cells 36
3.3.2 Staining 37
3.3.3 Measurement 37
3.4 Live Cell Based Assay 38
3.4.1 Sample Preparation 38
3.4.2 Cell Seed and Transfection 38
3.4.3 Antibody Staining 38
3.4.4 Flow Cytometry Measurement 39
3.5 Isotype Testing 39
3.6 Statistical Analysis 40
3.6.1 Delta MFI and MFI Ratio Calculation 40
3.6.2 Cut- off Value Determination 41
3.6.3 Data Analysis 41
Chapter 4: Results 42
4.1 A Live Cell Based Assay Optimized to Detect Anti-OMGp Antibodies 42
4.1.1 Outcomes of Transfection Optimization 42

4.1.2 Optimization of Staining 45
4.1.3 Voltage settings that give the best measurement 46
4.2 The Features of Study Cohort 47
4.3 Anti-OMGP Could Be Found in Serum but not in CSF. 48
4.3.1 The Criteria to Called an " Anti-OMGP Positive Patient" 48
4.3.2 Anti-OMGP Positive Patients 49
4.4 Autoantibodies Targeting anti-OMGP in Patients with Atypical Demyelinating Diseases 50
4.5 The IgG3 Isotype identified in Only One Patient 51
Chapter 5: dıscussıon 55
Chapter 6: Conclusion 59
Bibliography 60
Appendix A: SUPPLEMENTARY FIGURES 71

LIST OF TABLES

Table 3.1 Components of RF1 Buffer Solution. 33

Table 3.2 Components of RF2 Buffer Solution. 33

Table 3.3: Double Digestion Reaction of pOMGP-TM-GFP or pEGFP-N1 Plasmids by HINDIII and XHOI 35

Table 3.4 Scaling DNA concentration up/down to 0.75 µg or 1 µg, assuming a starting cell count of 200.000. 37

Table 3.5 Voltage settings for flow cytometry measurement by the Attune NxT device. 37

Table 3.6 The Optimized Voltage Settings for Attune NxT. 39

Table 3.7 Antibodies used in isotyping experiments. 39

Table 3.8 Cut-off Value Determination 41

Table 4.1 GFP transfection percentage rates obtained by flow cytometry in HeLa cells transfected with pOMGp-TM-GFP and pEGFP-N1.. 42

Table 4.2 GFP transfection percentage rates obtained by flow cytometry in HEK293 cells transfected with pOMGp-TM-GFP and pEGFP-N1. 43

Table 4.3 HeLa cell density and FUGENE:DNA ratios decided by GFP ratio 44

Table 4.4 Results of the experiment for different detachment methods. 45

Table 4.5 Optimization results of Alexa Fluor 647-conjugated Streptavidin antibody. 45

Table 4.6 22H6 positive control antibody optimization outputs. 46

Table 4.7 Primary characteristics of the patient cohort whose serum was studied. 48

Table 4.8 Primary characteristics of the patient cohort whose CSF was studied. .. 48

Table 4.9 Primary characteristics of the anti-OMGp positive patients 50

Table 4.10 Clinical Features of anti-OMGp-IgG Positive Patients. 52

LIST OF FIGURES

Figure 2.1 Demyelinating disease classification based on the affected area. …..... 6

Figure 2.2 Demyelinating disease classification based on its pathogenesis. 7

Figure 2.3 Multiple Sclerosis classifications and disease durations.. 8

Figure 2.4 Demyelinating Disease Types of the CNS. 21

Figure 2.5 Chromosome Location of the OMG gene at the NF1 locus on chromosome 17. 22

Figure 2.6 Schematic illustration of the immature (a.) and mature (b) structures of OMGp. 24

Figure 2.7 Schematic representation of OMGp protein three-dimensional structure.. 25

Figure 2.8 Relations of the prototypical myelin-associated inhibitors (OMGp, Nogo-A, and MAG) with their receptors.. 27

Figure 2.9 Representation for the experimental workflow of live cell-based assay. 30

Figure 4.1 The plate outline used at three different cell densities.. 42

Figure 4.2 Quantification of pOMGp-TM-GFP & pEGFP transfected cells incubated with 22H6 antibody then measured by flow cytometry at different voltage settings.. ... 47

Figure 4.3 Sample of negative and positive patient graphs. 49

LIST OF SUPPLEMENTARY FIGURES

Appendix A Figure 1 : Visualization of diagnostic digestion outcomes with the Gel Doc XR+ Imaging System.. 71

Appendix A Figure 2 : Optimization results of Alexa Fluor 647-conjugated Streptavidin antibody. 72

Appendix A Figure 3 : Measurement of 22H6 antibody tested at different dilution factors by flow cytometry. 73

Appendix A Figure 4 The pilot study for IgG1 antibody. 74

ABBREVIATIONS

aa	Amino Acids
ADEM	Acute Disseminated Encephalomyelitis
APS	Area Postrema Syndrome
AQP4	Aquaporin-4
AQP4 IgG	Aquaporin-4 Antibodies
AQP4-IgG (+) NMOSD	AQP4 Positive Neuromyelitis Optica Spectrum Disorder
AZA	Azathioprine
CCE	Cerebral Cortical Encephalitis
cDNA	Complementary DNA
CIS	Clinically Isolated Syndrome
CNS	Central Nervous System
CR	Cysteine-Rich
CRMP5	Collapsin Response Mediator Protein 5
CSF	Cerebrospinal Fluid
DEM	Disseminated Encephalomyelitis
DMEM	Dulbecco's Modified Eagle Medium
DMSO	Dimethyl Sulfoxide
DNA	Deoxyribose nucleic acid
EAE	Experimental Autoimmune Encephalomyelitis
ELISA	Enzyme Linked Immunosorbent Assays
EMG	Electromyography
FBS	Fetal Bovine Serum
GC	Glucocorticoid
GFAP	Glial Fibrillary Acidic Protein
GFP	Green fluorescent protein
GPI	Glycosylphosphatidylinositol
HEK293	Human Embryonic Kidney 293
HeLa	Henrietta Lacks Cells
IDD	Inflammatory Demyelinating Diseases
IgG	Immunoglobulin G

IL-6	Interleukin-6
IVIg	Intravenous Immunoglobulin
IVMP	Intravenous Methylprednisolone Pulse
kDa	Kilodalton
L-CBA	Live Cell-Based Assays
LETM	Longitudinally Extensive Transverse Myelitis
LINGO-1	Leucine-Rich Repeat and Ig Domain Containing 1
LRR	Leucine-Rich Repeats
mAbs	monoclonal antibodies
MAG	Myelin-Associated Glycoprotein
MAI	Myelin-Associated Inhibitor
MFI	Mean Fluorescence Intensity
MOG	Myelin Oligodendrocyte Glycoprotein
MOGAD	MOG-Antibody Associated Disease
MOG-IgG	Myelin Oligodendrocyte Glycoprotein Antibodies
MRI	Magnetic Resonance Imaging
MS	Multiple Sclerosis
NF1	Neurofibromatosis Type 1
NgR1	Nogo Receptor-1
NMDAR	N-methyl-D-Aspartate Receptor
NMO	Neuromyelitis Optica
NMOSD	Neuromyelitis Optica Spectrum Disorder
NogoA	Neurite Outgrowth Inhibitor
NSC	Neural Stem Cell
OCB	Oligoclonal Bands
OCT	Optical Coherence Tomography
OMGp	Oligodendrocyte Myelin Glycoprotein
ON	Optic Neuritis
OND	Other Neurological Disorders
p75NTR	P75 Neurotrophin Receptor
PBS	Phosphate Buffered Saline
PirB	Paired Immunoglobulin-Like Receptor B

PLEX	Plasma Exchange
PNS	Peripheral Nervous System
PPMS	Primary Progressive MS
RIS	Radiologically Isolated Syndrome
ROCK	Rho-Associated Kinase
RRMS	Relapsing-remitting MS
RT	Room Temperature
S/TR	Serine/Threonine-Rich
SAID	Systemic Autoimmune Disorders
SD	Standard Deviation
SPMS	Secondary Progressive MS
TM	Transverse Myelitis
WB	Western Blot
Δ MFI	Delta MFI

Chapter 1:
INTRODUCTION

1.1 Overview

Inflammatory demyelinating diseases (IDD) are a subgroup of demyelinating diseases and are a comprehensive class representing a range of heterogeneous conditions affecting the central nervous system (CNS). Multiple sclerosis (MS) with its variants is the most studied or encountered demyelinating condition of the CNS under this group. Although pathology or improved specific diagnostic criteria of MS can be beneficial in distinguishing it from other imitative reasons in patients with an atypical presentation, it is insufficient, and MS remains a first-thought clinical diagnosis for most cases and causes misdiagnosis. For instance, historically, Neuromyelitis Optica Spectrum Disorder (NMOSD), which is now a distinct disease entity, was believed to be a variant of MS until identifying autoantibodies directed against Aquaporin-4 (AQP4-IgG) in the serum of NMOSD patients has significantly facilitated the distinction from MS or others. Furthermore, with the myelin oligodendrocyte glycoprotein autoantibodies (MOG-IgG) detection in a subset of demyelinating diseases, a disease entity with its clinical heterogeneity separates from MS and AQP4-IgG positive NMSOD (AQP4-IgG + NMSOD) which is called MOG-antibody associated disease (MOGAD) has been specified.

Especially considering the last two decades, identifying specific disorders associated with autoantibodies like those AQP4-IgG+NMOSD and MOGAD has radically altered the definition of the international concept of IDD of the CNS. That emphasizes the importance of autoantibodies, which play significant roles in various encephalopathies and inflammatory conditions of the CNS. The autoantibodies are prospective biomarkers that specifically uncover and clarify a further disease entity of CNS-IDDs previously categorized as MS. Thus, the discovery of such autoantibodies makes it possible to make the proper diagnosis of many patients who cannot be explicitly diagnosed or misdiagnosis due to their atypical features and therefore to continue with appropriate treatment options.

The "gold standard" technique in tracing and detecting autoantibodies is undoubtedly live cell-based assays. The development of highly sensitive and precise cell-based assays has authorized us to define MOGAD disease in the literature as a distinct clinical

phenotype, while the classical methods, such as Western Blot (WB) or Enzyme-Linked Immunosorbent Assays (ELISAs), have been inadequate to detect MOG-IgG in patients. This situation highlights the requirement for the right laboratory bioassays to appropriate evaluation and implementation of prospect biomarkers.

While there are well-characterized and studied antibody biomarkers such as AQP4-IgG and MOG-IgG, there are various ones that have been recently introduced into the literature such as N-methyl-D-aspartate receptor antibody or dopamine-2 receptor antibody (Amatoury et al., 2013), Glial Fibrillary Acidic Protein (GFAP), Collapsin Response Mediator Protein 5 (CRMP5) (Greco et al., 2023) and are associated with new disease entities (e.g., GFAP-IgG associated Optic Neuritis, CRMP5- IgG associated Optic Neuritis). Many autoantibody candidates, such as oligodendrocyte myelin glycoprotein (OMGp), are waiting to be revealed. OMGp protein is explicitly expressed on the myelin surface of the oligodendrocytes and neurons at CNS. OMGp has the potential to be pathogenic due to that accessible localization, just like the MOG protein. These novel antibody biomarkers are promising for enhanced diagnosis, attention, and unlocking treatment options, specifically for atypical demyelinating CNS syndromes.

1.2 Aim & Hypothesis

Although most CNS demyelinating diseases seem to be related to each other, they differ from one another with distinct nuances that still need to be identified or are being discovered. Distinguishing between these diseases is crucial, especially regarding correct diagnosis and appropriate treatment. Uncovering anti-AQP4 and anti-MOG antibodies has significantly expanded the spectrum of demyelinating diseases and guided clinicians to accurately identify diseases like MS but different from MS. However, many patients still cannot be diagnosed due to their atypical features and the autoimmune target antigen of those atypical demyelinating diseases is still unknown. In a study published in 2020 (Gerhards et al., 2020), antibodies against oligodendrocyte myelin glycoprotein (anti-OMGp) were detected in the serum of some patients, mostly MS patients, and it was reported that these antibodies exhibited pathological effects in animal experiments which makes this protein as a new autoimmune target.

Nevertheless, it is yet unidentified whether anti-OMGp antibodies are associated with demyelinating diseases other than MS, especially those demonstrating atypical

characteristics. Therefore, that thesis hypothesizes whether patients not fully diagnosed due to their atypical features despite being in the defined group of CNS autoimmune diseases may have different disease entities related to their OMGp autoantibodies. Considering also that no tests have been performed to screen for OMGp antibodies in our country to date, the main objectives of the thesis are as follows:

i. Establishing a live cell-based assay in our laboratory to test OMGp autoantibodies,
ii. Screening for anti-OMGp antibodies across a diverse and large cohort of demyelinating diseases via this assay,
iii. Describe the clinical and radiological characteristics of the anti-OMGp antibody-associated disease.

Chapter 2:
LITERATURE REVIEW

2.1 Introductory Concepts: Myelination, Demyelination, and Remyelination

Myelin is the essential component and specialized insulating layer for many but not all axons in the CNS and the peripheral nervous system (PNS). The myelin sheath, composed mainly of lipids and proteins, occurs because of “myelination, " a complicated process involving the differentiation of specialized glial cells, known as oligodendrocytes in the CNS and Schwann cells in the PNS. Myelin is crucial for axon maintenance and function as it plays a role in efficiently transmitting electrical signals along the axons of neurons by enabling “saltatory conduction," acting as an insulator, reduces the metabolic energy required for the neuron to function so maintaining the strength and speed of nerve impulses (Adams & Kubik, 1952).

The significance of the integrity of the myelin sheath is underlined in the variety of diseases where impaired myelination is the core issue. Impaired myelination, which can be called “demyelination”, is the process where existing myelin sheaths are damaged and lost, it is one of the major causes of neurological disorders. Several mechanisms, including inflammatory or metabolic causes as well as genetic mutations affecting glial cells, can cause initial demyelination. Nonetheless of its reason, myelin loss induces

notable nerve dysfunction by delayed or blocked nerve conduction, resulting in injured communication networks between the brain and the body or within the brain. After demyelination, axons can be re-covered with novel myelin, typically slimmer and shorter than the first myelination, through “remyelination”, which is linked to functional rescue. However, in some cases, remyelination does not occur, generating axons and neurons to be susceptible to degeneration, resulting in various neurological symptoms for patients with demyelinating diseases (Franklin & Ffrench-Constant, 2008).

2.2 Demyelinating Diseases

Demyelinating diseases are a bunch of white matter disorders characterized by the alteration of myelin, which can occur due to numerous factors such as (i.) infective: a viral or bacterial infection, (ii.) genetic predisposition, (iii.) inflammatory: inflammation from an autoimmune disorder, (iv.) ischemic or toxic in source: other medical conditions such as vitamin defects or brain oxygen loss (Love, 2006). The signs or symptoms of demyelinating diseases differ based on the types but mostly involve neurological symptoms such as vision impairment, bladder or bowel problems, trouble walking or loss of coordination, muscle weakness or stiffness and spasms, and sensation or fatigue. Typical types of demyelinating diseases can be classified according to whether they affect the CNS or PNS (**Figure *2.1***). It is even possible to classify it according to its pathogenesis into several categories: immune-mediated inflammatory procedures, viral demyelination, demyelination caused by toxic or metabolic, and mechanical demyelination due to focal compression (**Figure *2.2***). Some of these differences are straightforward in that there is overlapping in pathogenesis between the entities in the distinct categories. However, classification provides a conceptual structure that may benefit proper diagnosis.

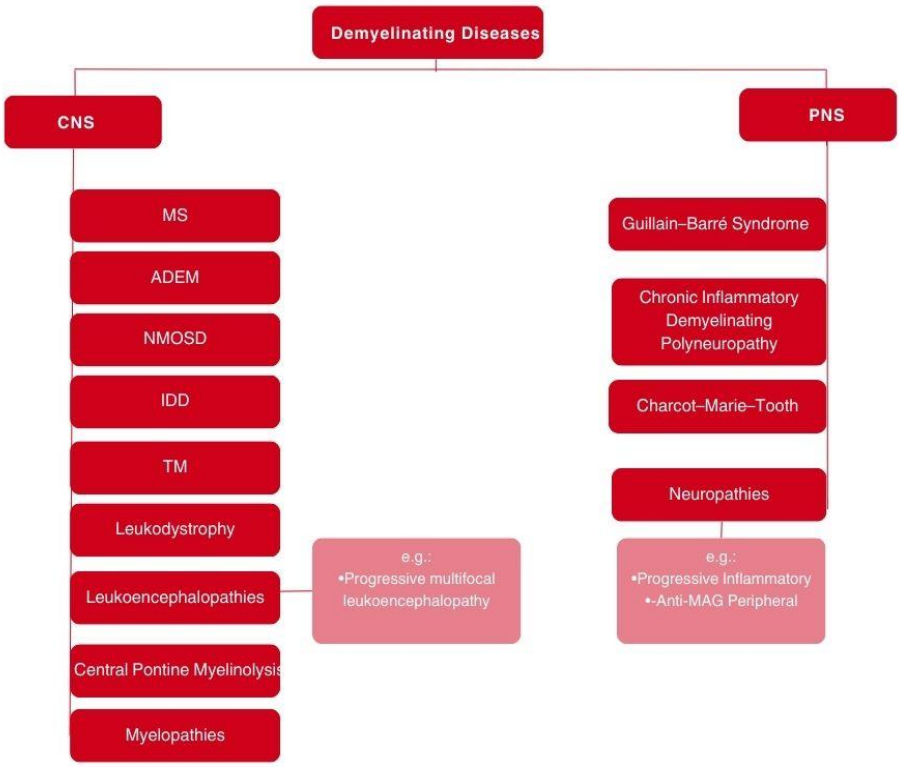

Figure 2.1Demyelinating disease classification based on the affected area. Light-colored boxes represent examples for the relevant subclasses: Progressive multifocal leukoencephalopathy for leukoencephalopathies and Progressive Inflammatory or Anti-MAG.

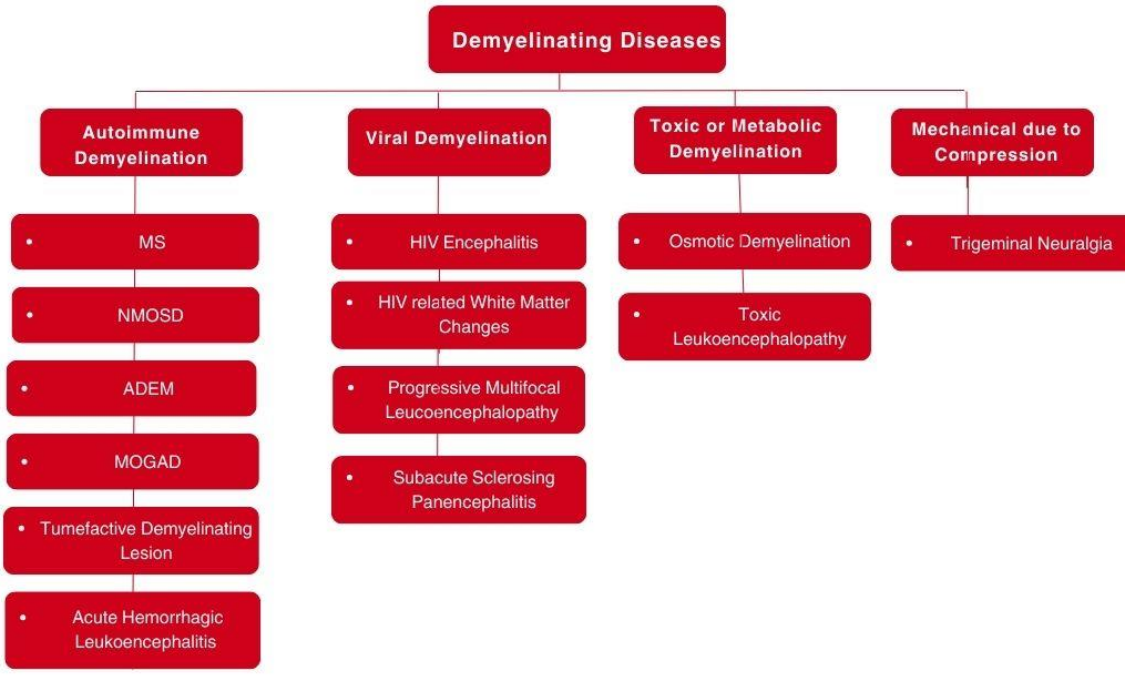

Figure 2.2 Demyelinating disease classification based on its pathogenesis.

Diagnosing demyelinating diseases is done through clinical and neurological examinations, where the patient's history is taken with the diagnostic criteria established for each type of demyelinating disease. Some tests such as Magnetic resonance imaging (MRI) scans, Spinal tap, Optical coherence tomography (OCT), Electromyography (EMG), Evoked potentials tests, cerebrospinal fluid (CSF) analysis, and blood tests also accompany the evaluations to exclude other conditions with overlapping symptoms.

2.3 Demyelinating Disease Types of the CNS

As mentioned just above, since the demyelinating diseases enclose quite large and various classes, only detailed theoretical information of the disease types available in our study will be included here.

2.3.1 Multiple sclerosis (MS)

MS is a chronic autoimmune disorder due to immune attacks targeting myelin sheaths wrapping nerve fibers of axons in the CNS, including both the brain and spinal cord, and is characterized by inflammation, demyelination, and neurodegeneration. According to Multiple Sclerosis Atlas, around 2.8 million individuals globally are affected by MS (Walton et al., 2020). Although MS can occur in people of all ages, it appears primarily in young adults between 20 and 30, and it is more likely to be seen in women than in men, with a women-to-male ratio of approximately 3:1. However, the prevalence of MS varies significantly across diverse geographical regions and populations, different than by sex and age and affected by other genetic or environmental risk factors. Obesity, Vitamin D deficiency, viral infections like Epstein–Barr virus infection or Tobacco exposure and smoking; as environmentally, certain alleles in the human leukocyte antigen or variants of the interleukin-2 receptor alpha gene (IL2RA) and interleukin-7 receptor alpha gene (IL7RA); as genetically could be given as examples for risk factors (Pérez, 2021; Waubant et al., 2019). The etiology of MS is not fully known yet, but all these factors can affect the immune system as a trigger or exacerbation of MS

to contribute to the disorder's evolution and progression, making the pathogenesis of the disease complex.

MS patients usually show a range of symptoms, which vary according to the intensity, zone, and degree of inflammation and the distribution of demyelinating plaques in specific anatomical regions. These regions include the brainstem, cerebellum (involved in balance and coordination), spinal cord, optic nerves, and the white matter surrounding the brain's ventricles (fluid-filled cavities)—the heterogeneity in plaque distribution results in diverse symptomatology among these patients (Eva et al., 2023). Common clinical presentations include visual impairments, motor and sensory dysfunctions, fatigue, cognitive decline, and atypical manifestations such as dysarthria and ataxia. However, MS can appear differently and be classified in 3 primary clinical forms: (i.) Relapsing-remitting MS (RRMS) is characterized by episodic attacks (relapses) followed by periods of remission; (ii.) Primary Progressive MS (PPMS): marked by a gradual progression of neurological decline from onset, without initial relapses and remissions, and (iii.) Secondary Progressive MS (SPMS): initially begins as RRMS but transitions into a phase of continuous deterioration (

Figure *2.3*).

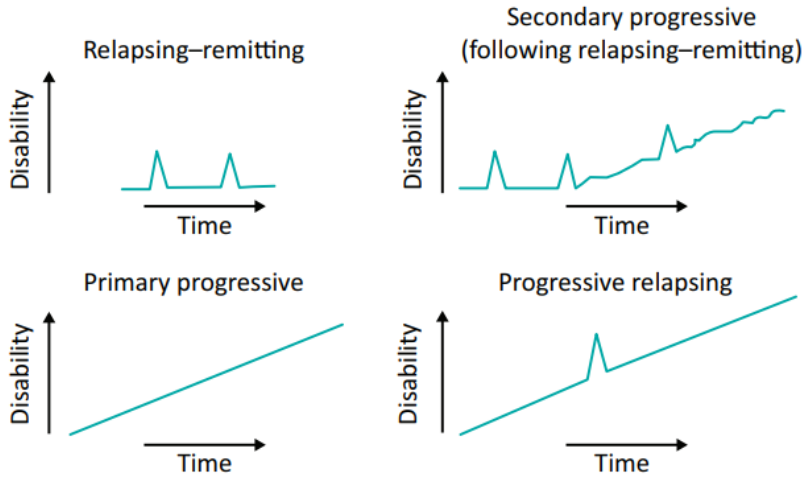

Figure 2.3 Multiple Sclerosis classifications and disease durations. Retrieved from "*Clinical Presentation and Diagnosis of Multiple Sclerosis*", by H. Ford, 2020.

The clinical progression observed in MS is associated with the cumulative neuro-axonal loss within a chronically inflamed CNS as well as an imbalance between ongoing damage, regenerative processes, and the functional reserve or resilience of the CNS (Woo, Engler, & Friese, 2024). While the progression of MS alters significantly among people, patients often experience clinical symptoms with complete or partial recovery, followed by periods of clinical stability and/or remission. In many cases, this condition can progress to RRMS, and finally, around one-quarter of patients may develop PPMS after a prolonged phase of disease evolution. Furthermore, most MS patients initially present with a clinically isolated syndrome (CIS) represented by a single demyelinating episode influencing the CNS for at least 24 hours without other conditions such as infections or metabolic diseases. Although the clinical and radiological findings suggest MS at the time of this first attack, the diagnosis is called CIS in a patient who does not fully meet the MS diagnostic criteria, and in most cases, CIS is considered the first condition to appear in patients who will develop MS. It should be considered that early therapeutic intervention can postpone long-term condition progression and ameliorate the consequences, which can be classified by the expanded disability status scale (EDSS). Thus, a proper diagnosis is crucial, particularly for patients with CIS who are at high risk of acquiring RRMS or PPMS.

The diagnostic criteria for MS appear to have improved remarkably since MS was first described as "La sclérose en plaques disséminées" and marked a triad of nystagmus, intention tremor, and scanning speech in 1868 by Charcot. After him, these initial criteria were supported by Poser criteria in 1983 with CSF analysis, MRI, and evoked potentials. With the increasing availability and utility of MRI, the International Panel on Diagnosis of Multiple Sclerosis developed the McDonald criteria in 2001, which gave greater emphasis to MRI findings to diagnose MS. These criteria have undergone several revisions, with updates in 2005, 2010, and the most recent in 2017, reflecting ongoing advancements in diagnostic methodologies and understanding of the disease (Ford, 2020).

The McDonald criteria, revised in 2017, are currently the most widely used for diagnosing MS. These criteria necessitate evidence of CNS damage, characterized by plaques in multiple areas or lesions appearing at distinct points or dissemination in time. Additionally, intrathecal IgG oligoclonal bands (OCBs) in CSF can replace the necessity for proven dissemination in time. However, these CSF analyses and additional tests, such

as evoked potentials and OCT, can provide supporting information but are generally optional for diagnosis. All these, together with the clinical history, neurological examination, and exclusion of other diagnostic options, are used to establish the diagnosis of MS (Maglio et al., 2024). The criteria aim to facilitate an early and accurate diagnosis of MS, thereby reducing uncertainty for patients and clinicians. Therefore, the diagnostic criteria are intended for patients with typical clinical presentations and should not be used in asymptomatic individuals with incidental MRI findings; such cases are categorized as radiologically isolated syndrome (RIS) (Ford, 2020). Misdiagnosis may lead to inappropriate treatment options and, therefore, cause more harm than good to patients, so it is vital to discriminate demyelinating disorders from each other.

Although there is no exact remedy for MS, various treatments or strategies are using focus on managing symptoms, reducing the frequency and severity of relapses, and slowing disease progression. Currently, disease-modifying therapies are the cornerstone of MS treatment and include immunomodulatory and immunosuppressive agents which are useful in intervening of the peripheral immune mechanisms that induce focal lesion formation, and with it decline clinical and radiological relapses. They nevertheless possess restricted achievement in stopping disease progression and diminishing rising disease activity (Woo et al., 2024). Hence, it is crucial to understand the disease mechanisms which would lead to the development of new therapeutic strategies, including personalized medicine, cell-based therapies, and gene therapy. Besides this, using the timeliness of diagnosis through the utilization of novel and appropriate biomarkers would aid in diagnosis and determining the optimal treatment strategies.

2.3.2 Neuromyelitis optica spectrum disorder (NMOSD)

NMOSD is a rare, relapsing inflammatory disease that affects the CNS, and it was thought to be a kind of MS disease called “neuromyelitis optica” (NMO) around up to two decades ago. Lennon et al., in 2004, a separate NMO-IgG serological marker targeting AQP4-IgG was detected in NMOSD cases for the first time (Lennon et al., 2004). The antibodies targeting the AQP4 water channel on astrocytes are a type of immunoglobulin G (IgG) directed in cooperation with complement system activation to target. The discovery of AQP4 has allowed a clear ‘seropositive’ description, with clearly indicated clinical characteristics in this group, and thus, NMOSD started to be classified

as a distinct disease entity. Because the AQP4-IgG is highly distinctive for NMOSD diagnosis and has a potential pathogenic function for disorder, for instance, it can induce attacks of the CNS by peripheral granulocytes via the CNS and activates complement-dependent cytotoxicity, antibody-dependent cellular cytotoxicity (mainly by natural killer cells), ultimate in astrocytic end feet damage, acute inflammation, secondary oligodendrocyte injury, and demyelination. However, it should be taken into consideration that not all NMOSD patients will have positive AQP4-IgG serology. Some NMOSD patients, defined as 'seronegative' NMOSD, meet clinical and radiological diagnostic criteria for the relevant disease but do not have anti-AQP4-IgG.

The diagnostic criteria and the knowledge about NMOSD have evolved quite significantly since the first description made by Eugene Devic and his student Fernand Gault in 1864. They defined a disorder as “neuromyelitis optica acuta" which is also known as Devic’s disease currently, and showed that it affects the optic nerve demyelination and the necrosis of an extended part of the spinal cord. (Jarius & Wildemann, 2013). Yet, diagnostic criteria for NMO were created for the first time in 1999, which mandated the presence of both optic neuritis (ON) and transverse myelitis (TM) corroborated by imaging studies and CSF findings (Weinshenker & Wingerchuk, 2017; Wingerchuk, Hogancamp, O'Brien, & Weinshenker, 1999).

However, these criteria were insufficient to separate NMO as a distinct disease from MS due to their matching clinical and radiological features until the discovery of AQP4-IgG in NMO in 2004. This identification led to the incorporation of AQP4-IgG positive serostatus into the 2006 diagnostic criteria as an auxiliary supportive marker. While both TM and ON remained essential for diagnosis, novel stipulations were added to the 2006 criteria, such as a positive AQP4-IgG serostatus, brain lesions that did not fulfill the diagnostic criteria MS, and MRI evidence of longitudinally extensive transverse myelitis (LETM) (Wingerchuk, Lennon, Pittock, Lucchinetti, & Weinshenker, 2006).

Then, in 2007, the term NMOSD was introduced to additionally encompass seropositive patients presenting with limited forms of the disease, so the potential phenotype was broadened. Finally, the last criteria version was published in 2015 by the International Panel for NMO Diagnosis (IPND) as "International Consensus Diagnostic Criteria." This standardized diagnostic terminology under NMOSD centers on AQP4-IgG as the primary diagnostic criterion and continues to be used for diagnosis today. According to this, at least one core clinical feature of NMOSD, along with positive serum

AQP4-IgG, is acceptable to diagnose AQP4-IgG-+ NMOSD. There are six core clinical qualities of NMOSD. These are (i.) Acute ON; (ii.) Acute TM; (iii.) Area postrema syndrome (APS) presenting with intractable nausea, vomiting, and/or hiccups; (iv.) Acute brainstem syndrome; (v.) Acute diencephalic clinical syndrome or symptomatic narcolepsy; (vi.) Symptomatic cerebral syndrome (Moheb & Chen, 2023). At least two core clinical features are required to diagnose AQP4-IgG seronegative NMOSD, with at least one being ON, TM, or APS, and additional MRI features like evidence of LETM.

Consequently, it can be said clearly that the detection of AQP4-IgG is at the center of these diagnostic criteria. The antibodies are currently most accurately assessed using patient serum via live cell-based assays (L-CBA). The detection of serum AQP4-IgG using L-CBA has demonstrated approximately 75% sensitivity and greater than 99% specificity, surpassing other methods such as ELISA. Hence, that assay is considered the gold standard for AQP4-IgG detection (P. J. Waters et al., 2012). In addition, principal techniques such as Neuroimaging and MRI and other tests such as OCT and visual evoked potentials are also used to determine other criteria for diagnosing NMOSD. According to all these, around 70-80% of NMOSD patients meet these criteria with seropositive AQP4-IgG, while a minority of patients have AQP4-IgG-negative disease. Seropositive NMOSD demonstrates a pronounced gender disparity, with a female-to-male ratio approaching 10:1, while the seronegative ones display an equal distribution between the sexes. The NMSOD typically manifests at a median age of 40 years. However, it can be present across a broad age range; up to 20% of cases are observed in individuals over 65 or pediatric patients (Siriratnam et al., 2023).

The majority of NMOSD patients experience a relapsing course of the disease, and predominantly, it is sporadic; nevertheless, rare familial cases have also been noted (Moheb & Chen, 2023). There are gradually accumulating disabilities irreversibly due to incomplete recovery following recurrent attacks. So, the prior goal of NMOSD treatments is symptomatically to control or prevent acute attacks and relapses, a substantial impact on health-related life quality, and possibly life-threatening effects. These remedies involved immunosuppressants (e.g., azathioprine (AZA) or mycophenolate mofetil) or glucocorticoids (GCs) until recently. Enhanced comprehension of NMOSD pathophysiology has revealed specific therapeutic targets such as B cell-depleting agents, Interleukin-6 (IL-6) receptor antagonists and complement inhibitors. As a result, since 2019, treatments by using monoclonal antibodies —eculizumab (anti-complement C5),

inebilizumab(anti-CD19), rituximab (Anti-CD20), tocilizumab and satralizumab (both are anti-IL-6 receptor), non-pathogenic anti-AQP4 and the most recent addition, ravulizumab(anti-complement C5)—have received approval for the management of AQP4-IgG (+) NMOSD (Preziosa et al., 2024).

2.3.3 Myelin oligodendrocyte glycoprotein antibody-associated disease (MOGAD)

MOGAD is an inflammatory demyelinating disorder of the CNS that is associated with structure-sensitive IgG autoantibodies targeting MOG which is unlike MS or AQP4-IgG (+) NMOSD. MOG is a glycoprotein located in the outer layer of oligodendrocytes as a compound of myelin sheath in the CNS and a member of the IgG superfamily due to its several splicing variants featuring extracellular IgG variable domains. The exact functional role of MOG is not fully understood; however, it is thought to take a role in cell-to-cell communication and regulation of complement-system response and contribute to the maintenance and structural integrity of oligodendrocytes-myelin. Due to its structural characteristics, like anatomical juxtaposition with the extracellular area, MOG has been extensively researched as an autoantigen capable of causing inflammatory demyelinating pathology in the CNS. Because it was thought that it has a probable role in interfacing with immune cells and strong antigenicity (Longbrake, 2022).

Due to its high antigenicity, MOG was previously thought to be a possible autoantigen for MS. More than one research study was done using WBor ELISA techniques that employ the denatured or linearized forms of the MOG protein to see if this argument is correct. The results demonstrated that MOG-IgG was not specific or pathogenic to any disorder since some of the general population, like patients with MS, other demyelinating CNS diseases, and healthy controls, have antibodies to the extracellular part of MOG. However, following studies revealed that MOG-IgG binds exclusively when the MOG protein is in its tridimensional structural form, which results in pathogenic, so the ELISA or WB is an inappropriate method for detection. Then, in 2007, O'Connor et al. displayed this structure-sensitive MOG-IgG firstly in patients with acute disseminated encephalomyelitis (ADEM) or ON but not found in MS by using MOG in its native protein form in laboratory assays (O'Connor et al., 2007). Thus, in recent decades, highly sensitive and specific L-CBAs using full-length naïve forms of human MOG, like AQP4-IgG detection assays, have been developed to detect MOG-IgG

in serum and CSF. These novel L-CBA methods (Spadaro & Meinl, 2016) have enabled the identification of MOG autoantibodies in patients with ADEM (Misu, Sato, Nakashima, & Fujihara, 2015), ON, TM and seronegative NMOSD (Kitley et al., 2012; Sato et al., 2014), brainstem, and cerebral cortical encephalitis(CCE) (Banks et al., 2020; Matsumoto et al., 2020) as opposed to the typical MS patients found mostly negative for MOG-IgG (P. Waters et al., 2015).

Consequently, this methodology, with other clinical and radiological manifestations, has facilitated the detection of MOG autoantibodies and proper identification of kids and adults with a demyelinating disorder different from MS and NMOSD called MOGAD, and the international diagnostic criteria of MOGAD were recently established by International Consensus Group. According to this criterion, to diagnose the patient with MOGAD, (i.) at least one of the core clinical demyelinating cases like ON, TM, ADEM, cerebral mono or polyfocal deficits, brainstem or cerebellar deficits or CCE, frequently with seizures must be present, (ii.) a clear-positive MOG-IgG L-CBA test result and (iii.) the exclusion of other diagnoses, including MS, are required (Banwell et al., 2023; Jarius et al., 2018) In the case of encountering a low positive result, which means that positivity without a reported titer or seronegative MOG-IgG with CSF positivity, further validating MRI or clinical evidence is critical for diagnosis. Present of; bilateral simultaneous clinical involvement, perineural optic nerve sheath enhancement, longitudinal optic nerve involvement (>50 per length of the optic nerve), and optic disc edema for ON; LETM, central cord lesion or axial H-sign on imaging for TM could be given as examples of such supportive features.

When considering all the clinical manifestations described in the criteria, studies have shown no sex-significant difference, and the core demyelinating cases in adult MOGAD patients are mostly ON or TM, whereas in pediatric MOGAD patients, ADEM with or without ON (Armangue et al., 2020; Cobo-Calvo et al., 2018; Hennes et al., 2017). This situation has shown that the condition's clinical phenotype predominantly relies on the patient's age, and MOGAD can arise in both adults and primarily children. However, the onset age is changeable, with a median of around the early to mid-thirties, and the disease could have a bimodal distribution. Pediatric patients define about 35% of cases, with an estimated incidence of around 3.1/1 million; a second peak could emerge in young/mid-adulthood (de Mol et al., 2020; Longbrake, 2022). So that MOGAD could have a monophasic or relapsing mode. Considering the prevalence of MOGAD, which is

approximately 1.3–2.5/100,000, and the annual incidence is approximately 3.4–4.8 per million (Hor & Fujihara, 2023), detecting anti-MOG-IgG utilizing L-CBAs is crucial for diagnosing accuracy, leading to the correct cure.

Although there is no currently approved definitive treatment option for MOGAD disease, various choices, such as acute management or long-term immunosuppressive therapy**,** are available depending on the progression and severity of the disease. For the acute phase management of MOGAD, most patients are treated with high-dose intravenous methylprednisolone pulse, which is a corticosteroid often supplemented with intravenous immunoglobulin (IVIg) and plasmapheresis, resulting in a generally promising response in 70–90% of patients (Di Pauli & Berger, 2018). So, patients with MOGAD show significantly better healing from seizures compared to those with anti-AQP4 positive NMOSD patients, who often require extra plasmapheresis. However, some patients may suffer severe, permanent disability, mainly resulting from the initial seizure. In such cases, earlier therapy might not be adequate, and patients could not respond to the treatment. Hence, they require alternative therapeutic options such as immunosuppressants (AZA, cyclophosphamide, tacrolimus, mycophenolate mofetil), satralizumab, or B cell depletion therapy (Stefan & Ciotti, 2024) . This long-term immunosuppressive therapy would decrease the risk of relapse and is vital to be continued since interrupting or ending treatment early has been associated with the progression of diseases.

2.3.4 Optic Neuritis (ON)

ON is an inflammatory optic neuropathy that predominantly affects the cranial nerve II, which is in transmitting nerve impulses from the retina to the lateral geniculate body located in the thalamus. In 2022, an international panel of physicians has been first described the diagnostic criteria for ON (Petzold et al., 2022). These criteria comprise a combination of clinical characteristics obtained from careful exams, history taking, and paraclinical tests. The clinical criteria encompass monocular, binocular impairment with or without orbital pain worsening on eye movements, reduced contrast and color vision, and a relative afferent pupillary defect. Additionally, at least a positive paraclinical test is required to confirm an ON diagnosis, such as OCT, MRI evidence, or humoral biomarkers, including serum antibodies to AQP4, MOG, or CSF-OCB.

ON is usually an earlier indication of CNS inflammation. It is characterized by the initial inflammation of this optic nerve, injury of the myelin sheath, and secondary damage to nerve fibers, causing the apoptosis and, so, death of retinal ganglion cells, which results in the probable vision impairment or/and loss (Del Negro et al., 2023). The reason for inflammation occurrence or being worse can be associated with various factors, including trauma, inflammatory conditions like vascular insufficiency, infectious agents, exogenous environmental factors like toxins, or autoimmune-mediated demyelination. There are also additional risk factors for ON, including obesity, smoking, MS, being of Caucasian descent, and residing in higher latitude regions. The prevalence of ON varies between countries, but it is estimated to be approximately 4–8 cases per 100,000/year globally (Braithwaite et al., 2020). However, ON affects females aged 20-40 years more than men. This entity is classified generally as "typical" or "atypical" entities, considering multifactor for the etiology of ON, some of which are mentioned above.

Typical and atypical groups of ON differ in clinical manifestation, findings from neuroimaging/MRI, response to cure, visual results, also biomarkers (Toosy, Mason, & Miller, 2014). Characteristic symptoms for typical ON contain retro-orbital pain on extraocular movements and acute unilateral vision loss because of an underlying demyelinating lesion. The typical ON is highly associated with MS as its sign, which determined in 20–42% of cases as manifesting symptoms or nearly half of patients with MS may develop ON during their disease course (Del Negro et al., 2023). However, it could also be idiopathic.

On the contrary typical ON, atypical ON is associated with a wide range of conditions, like NMO and NMOSD, autoimmune optic neuropathy, optic neuropathies from systemic disease (e.g. Sjogren's syndrome, sarcoidosis etc.), chronic relapsing inflammatory optic neuropathy (CRION), MOGAD, idiopathic neuro retinitis or other inflammatory/infectious/ autoimmune disorders out of MS. In addition to all these pathological disease states known to cause ON, there are also some rarer types of ON (medication-induced ON is referred to as toxic optic neuropathy- (TON)) caused by several drugs and risk factors, which are also contained in the atypical group. The atypical ON is characterized by deviations from typical symptoms, such as bilateral onset, painless extraocular movements but worse vision prognoses or the presence of optic nerve head/peripapillary hemorrhages. Moreover, the atypical etiologies could differ in the initial manifestation and severity, significantly influencing long-term visual

consequences. Mostly atypical ON has discordant visual recovery, while the typical ON prognosis is generally promising, with suitable visual recovery regardless of therapy. Therefore, differentiating between these various forms of ON and accurately diagnosing at presentation is essential and could enable the timely treatment of patients.

The recovery process from the ON typically proceeds through a sequential approach involving three main treatment methods: (i.) initial administration of intravenous GCs, followed by a sustained regimen of oral GCs, (ii.) plasmapheresis and (iii.) IVIg. These therapies may be utilized individually or in combination or be specific upon determining the patient's demographic characteristics (Bennett et al., 2023; Spillers et al., 2024). The approach to treatment could also change based on factors such as clinical manifestations, symptom severity, and etiological factors because of the diversity of underlying causes linked with ON.

2.3.5 *Transverse myelitis (TM*)

TM is a rare and pathologically heterogeneous syndrome characterized by immune-mediated neural injury across one or more spinal cord segments that leads to varying degrees of weakness, sensory deficits (e.g., numbness or tingling), and autonomic dysfunctions (bladder, bowel, and sexual) below the lesion site. The severity of these symptoms would alter depending on the scope and zone of the inflammation within the spinal cord; at peak deficit, half of TM patients are entirely paraplegic, with almost all the patients having a degree of bladder/bowel dysfunction (Krishnan, Kaplin, Pardo, Kerr, & Keswani, 2006).

Although the TM usually arises independently, it can also often be a complication of infection or part of the continuum of other neuro-inflammatory disorders. Therefore, the etiologies of TM can be widely categorized as parainfectious, paraneoplastic (e.g.: neurosarcoidosis and paraneoplastic syndromes), drug/toxin-induced, systemic autoimmune disorders (SAIDs), and acquired demyelinating diseases (Beh, Greenberg, Frohman, & Frohman, 2013). While MS, NMOSD, and ADEM are the most common acquired CNS autoimmune disorders associated with TM, the SAID --TMs mostly contain ankylosing spondylitis, antiphospholipid syndrome, Behçet disease, mixed connective tissue disease, rheumatoid arthritis, sarcoidosis, scleroderma, Sjögren syndrome, and systemic lupus erythematosus. On the other hand, Enteroviruses, herpes

viruses, Mycoplasma, Treponema pallidum, human T-cell leukemia type 1 (HTLV-1), and Zika virus are some of the causative examples of infections (Neri et al., 2018). Furthermore, noninflammatory etiologies (e.g., vascular, metabolic, neoplasms, nutritional etc.) can imitate TM's clinical and radiologic features.

Since many things could cause the occurrence of TM, as mentioned above, it is crucial to diagnose it correctly because an incorrect diagnosis can have severe consequences, such as choosing inappropriate treatment, which may not only be ineffective but could also exacerbate the underlying disease. According to the diagnostic criteria of TM, there are inclusion and exclusion criteria. The inclusion criteria consist of six points: (i.) onset or advanced of sensory, motor, or autonomic dysfunction linked to the spinal cord, (ii.) manifestation of bilateral signs and symptoms (though not necessarily symmetrical), (iii.) presence of a delineated sensory level, (iv.) exclusion of extra-axial compressive causes via neuroimaging (MRI or myelography; computed tomography (CT) scans are insufficient), (v.) confirmation of spinal cord inflammation through CSF pleocytosis, elevated IgG index, or gadolinium enhancement and (vi.) progression to the lowest point (nadir) occurring between 4 hours and 21 days after symptom onset. However, the exclusion criteria are contain three matters: (i.) the radiation therapy to the spine within the past decade, (ii.) presence of abnormal flow voids on the spinal cord's surface consistent with arteriovenous fistula and (iii.) clinical deficit in arterial distribution consistent with anterior spinal artery thrombosis ("Proposed diagnostic criteria and nosology of acute transverse myelitis," 2002; Simone CG, 2024).

The annual frequency of TM goes from 1.34 to 4.6 cases per million/year, expanding to 24.6 cases per million/year when MS or other acquired demyelinating diseases are enclosed. There is no gender/familial/ ethnic predisposition for TM; it can appear at any age. However, it has a bimodal peak (10-19 and 30-39) between ages 10 to 40 (Bhat, Naguwa, Cheema, & Gershwin, 2010).

To diagnose TM, clinical assessment, imaging examinations, and laboratory analyses are used. The MRI technique is mainly used for imaging the spinal cord, which is pivotal in pinpointing inflammation sites and excluding alternative causes such as spinal cord compression. Excluding a compressive cord lesion for diagnosing TM is essential, and this exclusion is generally made by using MRI. Additionally, the Lumbar puncture and analysis of CSF are used for diagnosis, which might reveal heightened white blood cell

counts or augmented protein levels that signify inflammation. Moreover, the blood assays serve to uncover underlying conditions or infections.

After a diagnosis of TM, the treatment should be started without delay, which aims to reduce inflammation and manage the symptoms. The gold standard and primary treatment for TM is intravenous GCs; prompt initiation of high-dose intravenous GCs is crucial to decrease spinal cord inflammation. Plasma exchange (PLEX) and intravenous IVIg therapy are options for patients who do not respond to steroids, especially for acute CNS-demyelinating diseases. Furthermore, with evolving knowledge of TM, immunomodulatory therapies like cyclophosphamide, mycophenolate, or rituximab may provide benefits. Long-term management would also be beneficial, including physical therapy, occupational therapy, and medications to manage symptoms like muscle spasms, pain, and bladder dysfunction.

2.3.6 Acute disseminated encephalomyelitis (ADEM)

ADEM, one of the types of autoimmune encephalitis, is an acute, immune-mediated, inflammatory demyelinating clinical syndrome of the CNS characterized by encephalopathy and multifocal brain lesions. Depending on the inflammation location, the ADEM can have numerous distinct symptoms, including fever, headache, vomiting, nausea, confusion and/or consciousness, and fatigue. According to the zone involved in the demyelinating process, the neurological manifestation would be associated with motor, sensory, and cognitive deficiencies, which might involve tingling or numbness in the arms and legs, problems in swallowing, vision deficits or/ loss (optic neuritis), aphasia, muscle weakness, trouble walking, altered perception of pain and temperature, etc. ADEM patients could furthermore show pyramidal dysfunction, hemiparesis, cerebellar ataxia and cranial nerve dysfunction.

The clinical diagnosis of ADEM can be challenging due to this clinical presentation being so heterogeneous and polyfocal onset largely as described above and the lack of biomarkers or diagnostic tests. Therefore, the diagnosis of ADEM is made using historical, clinical, and radiologic findings according to criteria revised in 2013 by the International Pediatric Multiple Sclerosis Study Group (IPMSG) (Krupp et al., 2013), and it is important to exclude other diseases before a definite diagnosis. According to these criteria, describing pediatric ADEM needs all of the following: (i.) an initial multifocal

clinical event in the CNS with a default inflammatory demyelinating reason, (ii.) encephalopathy that cannot be clarified by fever, (iii.) no recent clinical and MRI findings emerge≥3 months after the onset, (iv.) brain MRI is abnormal during the acute (3-month) phase; and (v.) generally on brain MRI: diffuse, borders are unclear, large (>1– 2 cm) lesions involving the cerebral white matter predominantly. Although it can be seen at any age, ADEM mainly affects children and young individuals following viral infection or immunizations. For this reason, it is also called "post-infectious encephalomyelitis" (Massa, Fracchiolla, Neglia, Argentiero, & Esposito, 2021), and since no alternative criteria are given in the adult population, these criteria are also used for adults in recent studies.

Majority of cases that defined as ADEM to this criteria are usually monophasic, while some ADEM patients with relapsing disorders such as recurrent DEM , multiphasic DEM, NMOSD, and MS have been reported (Santoro & Chitnis, 2019). This relatively rare condition has an estimated incidence of 0.5 per 100.000 with the median age of onset of between 5-9 years, and it does not have any ethnic or racial preference. Although most studies have indicated that the male-to-female ratio alters between 1:0.8 and 2.3:1, and male predominance has been shown, a dominant gender difference has not yet been defined (Paolilo, Deiva, Neuteboom, Rostásy, & Lim, 2020). With appropriate treatment, many patients, especially children, could recover fully.

Although the treatment approach varies from case to case, the therapeutic approach generally starts with first-line therapy. It continues with a secondary-line depending on the severity of the situation and finally with a long-term follow-up of physical and neurocognitive outcomes (Wang, 2021). First-line therapy includes high-dose steroids, most often methylprednisolone, to diminish inflammation for the control of acute ADEM. When the cases are severe or refractory to first-line treatment, concurrent or sequential PLEX and IVIg could be used as the second step. Long-term follow-up is necessary to observe for possible relapses or the development of other autoimmune diseases. Furthermore, due to ADEM being the most typical initial presentation of MOGAD, the existence or lack of MOG antibodies will also be important to addressing therapeutical strategies.

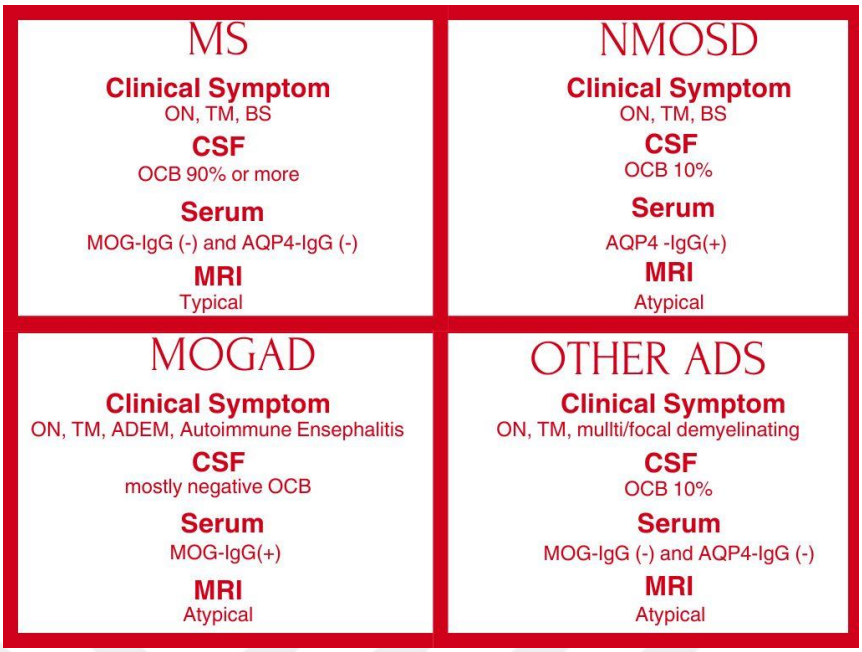

Figure 2.4 Demyelinating Disease Types of the CNS. Summary of the common types of CNS demyelinating disease types, including their clinical symptoms and specific characteristics. MS, multiple sclerosis; MOGAD, myelin oligodendrocyte glycoprotein-IgG-associated disorder; NMOSD, neuromyelitis optica spectrum disorder; ADS; acquired demyelinating syndrome; ON, optic neuritis; TM, transverse myelitis; ADEM, acute disseminated encephalomyelitis; BS, brainstem syndrome; CSF, cerebrospinal fluid; OCB, oligoclonal band; MOG, myelin oligodendrocyte glycoprotein; AQP4, Aquaporin-4.

2.4 Oligodendrocyte myelin glycoprotein (OMGp)

OMGp is the protein encoded by the OMG gene. This gene does not include any introns within the coding sequence and located on Chromosome 17q11.2 (Mikol, Alexakos, et al., 1990) (**Figure *2.5***) that is ingrained in the intron of neurofibromatosis type 1 (NF1) gene, a tumor suppressor gene, by extends over at least 2.7 kb of this genomic DNA with situated within 4 kb of the breakpoint of a balanced chromosomal translocation (Viskochil et al., 1991). The OMGp was initially discovered in CNS-myelin extract and characterized as peanut agglutinin-binding protein (Mikol & Stefansson,

1988) then was called as OMGp to indicate its specificity for the oligodendrocyte-myelin unit (Mikol, Gulcher, & Stefansson, 1990).

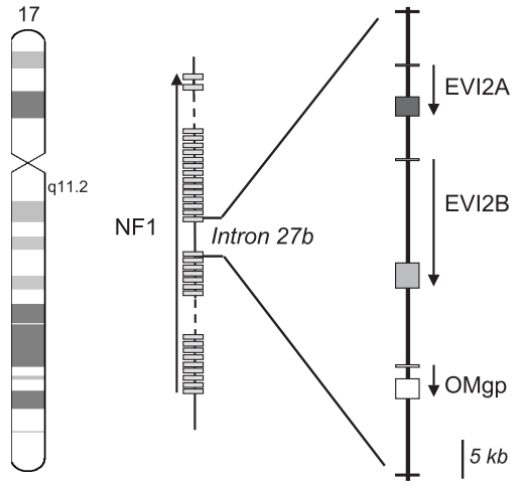

Figure 2.5 Chromosome Location of the OMG gene at the NF1 locus on chromosome 17. The OMG gene is embedded within intron 27b of the NF1 gene after the EVI2A and EVI2B genes. Arrows indicate the transcription direction. NF1, neurofibromatosis type 1; EVI2A, ecotropic viral integration site 2A; EVI2B, ecotropic viral integration site 2B. Sourced from *"Oligodendrocyte Myelin Glycoprotein (OMgp): Evolution, Structure and Function",* by P. Vourc'h, 2004.

2.4.1 Struction

Human genomic DNA library screening by using a clone of human OMGp cDNA, in 1990, allowed the primary structure of OMGp to be determined (Mikol, Alexakos, et al., 1990). That protein has two structures: the "immature" form and the "mature" form. The mature form of OMGp is formed, whereas the immature form of the OMGp undergoes a few minor modifications.

The immature OMGp

Figure **2.6** a.) comprises 440 amino acids (aa) sequences with four main domains following the leader sequence of 17 amino acids at the N terminal part. These are (i.) NH_2

terminus consisting of one short cysteine-rich (CR) motif (ii.) leucine-rich repeats (LRR), (iii.) serine/threonine-rich (S/TR) region, and (iv.) COOH (carboxylic acid)-terminal segment, which is hydrophobic. This hydrophobic site seems to be cleaved concomitant with the joining of glycosylphosphatidylinositol (GPI)-connection to the C-terminal in the mature form of OMGp (Mikol, Gulcher, et al., 1990; Vourc'h & Andres, 2004).

When the mature structure (

Figure 2.6 b.) is analyzed closely, the OMGp contains 401 aa sequences with four domains: (i.) a CR region on the N terminal site is probably involved in forming two disulfide bonds, and it comprises 32 aa-length and four cysteines, (ii.) an LRR domain with 172 aa-length sequences that includes eight sequential leucine-rich repeats, making the OMGp protein a member of the LRR protein family, (iii.) a S/TR region with 197 aa-length sequences and some sites that are supposed to fix O- linked carbohydrates, and (iv.) the GPI domain by which the OMGp protein is anchored to the external layer of the plasma membrane and is cleaved by phospholipases to release the soluble polypeptide form of OMGp (Vourc'h & Andres, 2004; Vourc'h, Moreau, et al., 2003). In addition, some sub-OMGP molecules have been demonstrated to possess the human natural killer cell antigen-1 carbohydrate which contains the sulfate-3-GlcA β1→3Gal β1→4GlcNAc fragment (Mikol, Gulcher, et al., 1990; Vourc'h & Andres, 2004).

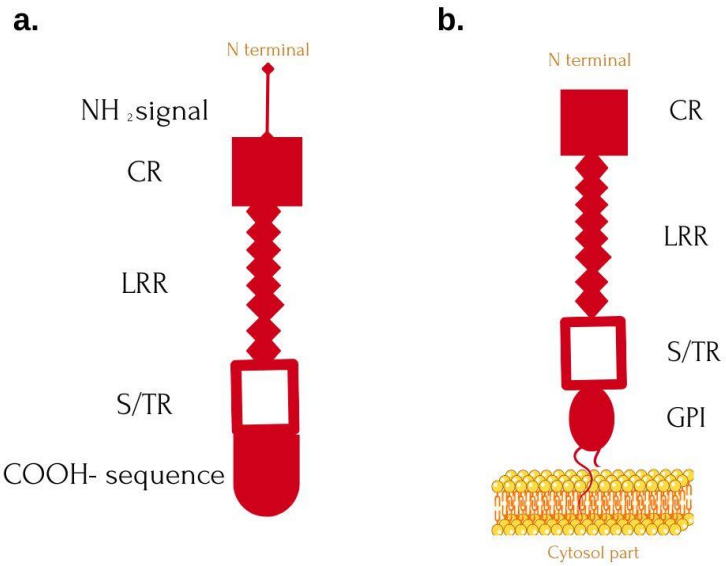

Figure 2.6 Schematic illustration of the immature (a.) and mature (b) structures of OMGp. Domains in the OMGp protein are CR, cysteine-rich domain; LRR, leucine-rich repeat domain; S/TR, serine/threonine-rich domain. GPI, glycosylphosphatidylinositol.

The most detailed studied structural part of the OMGp is LRR domain. For example, the three-dimensional structure of the LRR domain of OMGp was modeled by Vourc'h et al. using the Y. pestis YopMcytotoxin as a template of the structure. It was shown that this domain is the most conserved and supports its role as a protein-interacting or adhesion domain like in most other proteins in the LRR family via this model (Vourc'h, Moreau, et al., 2003).

On the other hand, the OMGp is a greatly glycosylated 120 kDa protein that is normally anchored to the cell membrane through a GPI mediator and could be released from the membrane as 105 kDa polypeptide in soluble form (Mikol & Stefansson, 1988). Mikol et al. showed that OMGp contains multiple O- and N-linked oligosaccharides when the deglycosylating enzymes are applied, which also aligns with its extracellular localization. According to these, N-linked carbohydrates contribute at least 25 kDa to OMGp's mass. Defining the quantity of O-linked carbohydrates proved challenging, but Mikol et al. reported OMGp's mass as approximately 52 kDa post N- and O-deglycosylations. Given that the GPI anchor accounts for 15 kDa, O-linked oligosaccharides are estimated to contribute around 30 kDa to OMGp's overall mass (Mikol & Stefansson, 1988). Besides that, it is also known that the molecular mass of the mature OMGp backbone polypeptide is about 46 kDa (Mikol, Gulcher, et al., 1990).

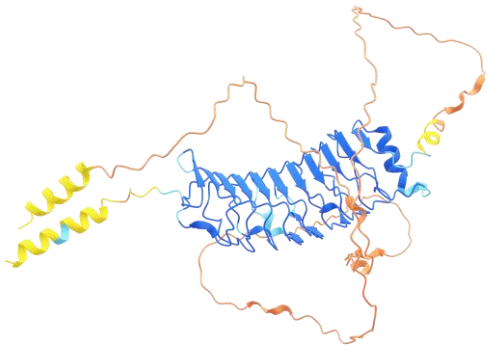

Figure 2.7 Schematic representation of OMGp protein three-dimensional structure. *Uniprot, Protein Code; P23515 · OMGP_HUMAN / Structure, 2024.*

2.4.2 Localization

The OMGp protein was isolated from CNS myelin at first (Mikol & Stefansson, 1988). During the developmental process, the expression OMGp exhibits a temporal correlation with CNS myelination. Precisely, it constantly elevates from the birth period to early adulthood, then decreases until it stabilizes at a consistent level in adulthood (Geoffroy & Zheng, 2014; Vourc'h, Dessay, et al., 2003). While it is believed to be localized in compact myelin at the outset, subsequent research revealed that OMGp is expressed in the membrane surrounding the Nodes of Ranvier, produced by oligodendrocyte-like cells(Huang et al., 2005). In line with this localization, they showed that nodal architecture is altered in OMGp-deficient mice, resulting in a notable accumulation of axonal sprouting from these altered nodes in vivo. However, another group has contested these results and demonstrated that the observed expression profile was due to the antibody's cross-reactivity with versican V2, thereby interrogating the perinodal distribution of OMGp (Chang, Susuki, Dours-Zimmermann, Zimmermann, & Rasband, 2010).

Despite its name indicating specificity to oligodendrocytes, the OMGp protein is also expressed by several neurons in addition to oligodendrocytes and localized at their myelin membranes (Miki et al., 2014). The OMGp of the developing cortex is located at the thalamocortical barrel area, on the exterior of neurons, in dendrites and axons, brain synaptosome fractions, and axon varicosities (Gil et al., 2010). Neurons from the hippocampus, cerebellum, brainstem, neocortex layer five, and spinal cord express OMGp in the adult CNS (Geoffroy & Zheng, 2014). The large projection neurons, hippocampal pyramidal neurons, and cerebellar Purkinje cells could be examples of these neuron types (Habib et al., 1998). The OMGp was also found to be expressed by astrocytes (Zhang et al., 2014).

2.4.3 Function

By far, the most studied and best-known function of OMGp is related to the inhibition of axonal regeneration/neurite outgrowth under the roof of myelin-derived growth inhibitory proteins. The first relationship between neurite outgrowth inhibition and OMGp was established in 2002 by Kottis et al. by finding that arretin, a protein fraction clarified from bovine brain myelin -called previously "arretin" due to this inhibitory capability, was composed mainly of OMGp (Kottis et al., 2002). Subsequently, OMGp was characterized as a myelin-associated inhibitor (MAI), like two other proteins, neurite outgrowth inhibitor (NogoA) and myelin-associated glycoprotein (MAG). Despite these three MAIs having no structural homology, they are usually referred to as the "prototypical MAIs" since they share joint receptors such as Nogo receptor-1 (NgR1), paired immunoglobulin-like receptor B (PirB and LILRB2 in human). They inhibit axon regeneration/ neurite outgrowth through a downstream signaling pathway employing Rho and Rho-associated kinase (ROCK) by binding to the NgR1, leucine-rich repeat GPI-linked protein (**Figure *2.8***). The inhibitory signals are transduced into the cell by tying to co-receptors with intracellular signaling domains, such as p75 neurotrophin receptor (p75NTR), TROY, leucine-rich repeat and Ig domain containing 1 (LINGO-1) (Xu, Wang, & Jin, 2015). OMGp binds to NgR1 by its LRR domain through the C-terminal region and becomes functioning, which was learned thanks to the alanine scanning mutagenesis for NgR1 and the domain deletion analysis for OMGp (Laurén et al., 2007; Saha, Kolev, & Nikolov, 2014). Thus, OMGp together with MAG and NogoA induces growth cone collapse, regulates the axon- myelin connections and mediating cell communications (specifically interaction between oligodendrocyte to oligodendrocyte or oligodendrocyte-axonal membrane at the nodes of Ranvier).

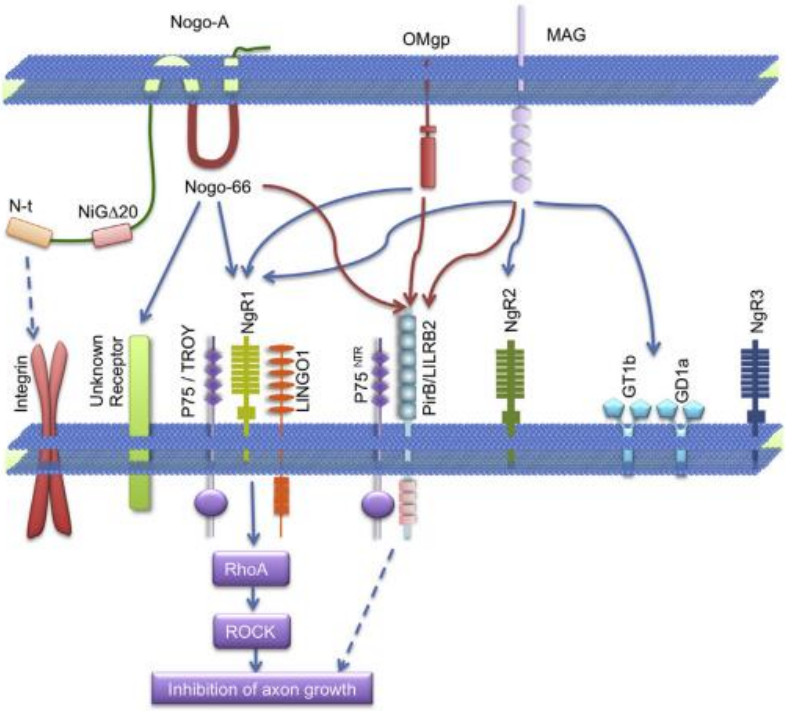

Figure 2.8 Relations of the prototypical myelin-associated inhibitors (OMGp, Nogo-A, and MAG) with their receptors. They inhibit axon outgrowth through a downstream signaling pathway employing Rho and Rho-associated kinase (ROCK) by binding to the Nogo receptor-1 (NgR1), paired immunoglobulin-like receptor B (PirB) receptors. Taken from *"Myelin-Associated Inhibitors in Axonal Growth after Central Nervous System Injury"*, by C.C. Geoffroy, 2015.

Three independent studies show that the genetically deleting OMGp did not promote corticospinal tract axon regeneration. In contrast, they demonstrated that it enhanced 5-hydroxytryptamine axon sprouting, confirming its synergetic role in inhibition of axon sprouting after CNS injury in vivo (Cafferty, Duffy, Huebner, & Strittmatter, 2010; Geoffroy & Zheng, 2014; J. K. Lee et al., 2010). Besides that, OMGp is essential in forming and maintaining myelin construction (Vourc'h & Andres, 2004). Nie et al. (Nie et al., 2006) showed that while overexpression of OMGp leads to the outgrowth of myelin. In a different study that would support these results and demonstrate the importance of the role of OMGp in myelination processes, it was found that OMGp-null mice were hypomyelination of the spinal cord that was associated with slower propagation of

afferent and efferent electrical impulses (X. Lee et al., 2011). In 2014, Miki et al. also indicated an improved myelination in the rats with elevated levels of OMGp and brain-derived neurotrophic factor (BDNF) (Miki et al., 2014).

OMGp could also have other functions distinct from neural regeneration or myelination since it plays various roles in injured immature and mature CNS. For instance, OMGp, expressed by neural stem cells (NSCs), could control cell proliferation during brain development due to its localization within the NF1 gene intron. Studies have shown that overexpression of the NF1 gene or OMGp has similar results, which enhances cell proliferation inhibition (Martin et al., 2009). They reached this result by showing that OMGp could decrease NSC proliferation by interacting with the NgR1 expressed by NSCs but does not impact the neuronal differentiation of the cells. Furthermore, another study also indicates that OMGp plays an active role during development and may impact axonal target specification during the establishment of thalamocortical connections in the developing cortex (Gil et al., 2010).

Beyond these, OMGp, just as NogoA or chondroitin sulfate proteoglycan (CSPG), has been associated with controlling synaptic plasticity (Karlsson, Wellfelt, & Olson, 2017; Raiker et al., 2010). Although it is present in both presynaptic and postsynaptic density fractions (Mironova & Giger, 2013), it functions postsynaptically in an NgR1-dependent manner rather than increasing the release of presynaptic neurotransmitters, regulates synapse generation and maturation, and impacts activity-dependent synaptic strength. In addition to these, some studies available in the literature suggest that OMGp may be one of the key molecules related to epilepsy. Interestingly, a study examining the relationship between the NgR1 pathway and epileptogenesis (He et al., 2021) showed that this pathway is particularly activated in the chronic phase of epilepsy and is characterized by upregulation of OMGp along with NogoA, MAG, and LINGO-1 during epileptogenesis. Another study conducted much earlier than this study (Hu et al., 2016) demonstrated that the expression of myelin-related proteins such as OMGp, myelin basic protein (MBP), and MAG decreased in epileptic foci due to demyelination.

Recently, the presence of autoantibodies against OMGp was demonstrated in a group of patients, mainly with MS, (Gerhards et al., 2020) and it was suggested that OMGp could be an autoantigen, especially for MS (Quagliata et al., 2023). Finally, OMGp has been shown to stimulate the NGR1 pathway by needing the Rho guanine nucleotide exchange factor Kalirin-9 and RhoA activation in the dendrite increased upon this

stimulation (Grubisha et al., 2021). Furthermore, they showed that when RhoA activation is inhibited, the effect of OMGp stimulation on dendritic architecture is blocked. Considering this, they suggested that OMGp plays an influential role throughout adolescence and into adulthood, possibly acting in typical dendritic growth restriction and stabilization.

2.5 Live Cell Based Assay to Detection of Autoantibodies

Classical methods such as ELISA and/or WB have been widely used to detect autoantibodies in sera associated with autoimmune disorders of the CNS so far. However, the inadequacy of these methods in recognizing extracellular or surface epitopes with the possibility of an immunoreactive reaction with intracellular antigens and the fact that antibodies binding to the extracellular domain of the proteins are inclined pathogenic have been parturition the need for more accurate and sensitive novel assays. Cell-based assays, currently defined as the field's "gold standard"(Reindl et al., 2020; Yeh & Nakashima, 2019), have emerged in line with this requirement, and it played a significant role in associating AQP4 antibodies with NMOSD and MOG antibodies with MOGAD disease, leading to the identification of distinct disease entities from MS and others.

In short, the method ,which shown in (**Figure *2.9***),entails the expression of an epitope or antigen of interest on the surface of mammalian cells, typically human embryonic kidney 293 (HEK293) or Henrietta Lacks (HeLa) cells, in its native form mostly by transfecting vectors carrying the complete cDNA sequence of the target antigen. This unique overexpression of the antigen makes the test specific. Then, these non-permeabilized live cells are incubated with patient serum, which is diluted before at the determined dilution factor, followed by a fluorochrome-conjugated anti-human IgG secondary antibody. The fluorescence intensity is subsequently measured by microscopy or flow cytometry, indicating the level of autoantibody binding. However, the flow cytometry is more favorable than other visualization techniques because it is quantitative (quantification is made via the calculations between serum binding to antigen-expressing cells and control cells, using either subtraction (delta) or division (binding ratio)), not investigator-dependent, and does not utilize radioactive (Amatoury et al., 2013). Even Waters et al. compared various antibody detection methods, including cell-based assays

followed by microscopy or flow cytometry analysis or depending on live cells or fixed ones (P. J. Waters et al., 2019). They also showed that the flow cytometry live-cell-based assay was the most sensitive, accurate, and trustworthy procedure. In addition, these tests are beneficial as they make it easier than classical ones to screen a large cohort in a short time.

As a result, this essential test, which has the potential to mediate the discovery of specific antibodies that could be biomarkers that may be associated with different diseases, is currently used for diagnostic purposes as the gold standard in identifying various diseases such as MOGAD and AQP4 (+) NMOSD. Furthermore, its results are more satisfactory than using assays utilizing fixatives or other classical techniques.

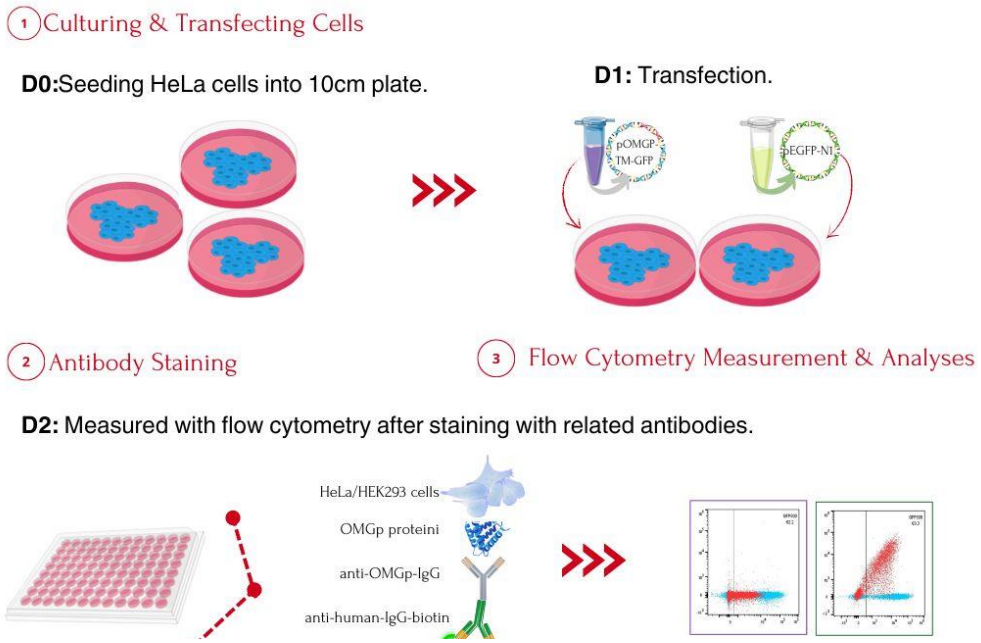

Figure 2.9 Representation for the experimental workflow of live cell-based assay. After 24 hours of seeding cells, transfections are made using pOMGp-TM-GFP (purple) and pEGFP-N1(green) plasmids. Day after, staining is conducted after serum/ cerebrospinal fluid incubations by using anti-human-IgG-biotin, Alexa Fluor 647-conjugated streptavidin, and Propidium Iodide, respectively, to detect anti-OMGp autoantibodies at transfected cells. Subsequently, the measurements are accomplished via Attune NxT device using flow cytometry technique.

2.6 Autoantibodies Against anti-OMGp

In 2020, Gerhards et al. published a study that is the only one in the literature showing that OMGp antibodies have a pathogenic potential and can be detected in different inflammatory CNS disease groups (Gerhards et al., 2020). In that study, which sought to investigate whether OMGp would be a candidate as an autoimmune target, they first developed a rigorous L-CBA with membrane-anchored OMGP. Screening patients with inflammatory CNS diseases via this assay and determining a strict cut-off value, they detected 10 (2.3% MS and 3.6% ADEM) positive patients out of 474, while all 114 healthy controls were negative. After identifying autoimmunity to OMGP, they also investigated the pathogenic effects of that autoimmunity in the experimental autoimmune encephalomyelitis (EAE) model with OMGP-specific T cells and/or monoclonal antibodies (mAbs). In this way, they firstly showed that OMGP-specific T cells generate a unique form of EAE characterized by infiltrations in the meninges around the cortical convexities; secondly, unlike anti-MOG mAbs, anti-OMGP mAbs did not cause demyelination or other tissue impairment in the EAE model. Instead, they proposed that OMGP-specific T cells open the blood-brain barrier and pave the way for demyelination by MOG-Abs, providing an animal model for lesion localization of OMGP-driven autoimmunity. Thus, OMGp mAbs were defined as novel pathogenic targets that could be included in future antigen cocktails.

Chapter 3:
METHOD

3.1 Plasmid Obtaining

3.1.1 pOMGP-TM-GFP & pEGFP-N1 plasmid Elution

Plasmid DNAs were recovered from filter paper by cutting out of the circles containing DNA using a sterile razor blade, putting those pieces into sterile Eppendorf tubes carefully, mixing a well of 10-15 µL Elution Buffer onto the circle, then centrifuged at 4000 rpm for 10 seconds. The eluted DNA concentration was checked via NanoDrop

2000c (Thermo Scientific) measuring. Then, as described below in 3.1.4 section, 2 µL of each DNA was transformed into competent bacteria.

3.1.2 Bacterial Growth Medium Preparation

a) To prepare Tryptic Soy Agar (Sigma, #22091-500G), 40 g of dehydrated media was suspended in 1 liter of purified filtered water, then sterilized at 121°C for 15 minutes and cooled to 45- 50°C. After mixing well with the desired antibiotic or without antibiotic, it was appropriately dispensed into sterile Petri dishes.

b) To prepare Tryptic Soy Broth (Sigma, #22092-500G), 30 g of dehydrated media was suspended in 1 liter of purified filtered water, sterilized at 121°C for 15 minutes, cooled to 45- 50°C, and mixed well with the desired antibiotic at the proper ratio.

3.1.3 Competent Bacteria Preparation

Initially, the STBL3 strain of E. coli from lab stocks was spread on an antibiotic-free LB agar plate and incubated at 37°C for 16-18 hours to allow colony formation. A single colony was picked from that plate and grown overnight in 3 mL of LB-broth at 37°C with shaking at 225 rpm. Approximately 16-18 hours later, 1 mL of this culture was transferred into 100 mL of fresh LB- broth. This bacterial culture was then incubated at 37°C on a shaker until the bacterial suspension's optic density (OD600) reached 0.4 (0.4-0.55 optimum) to ensure the bacteria reached the logarithmic growth phase, indicated by cell doubling. When the OD600 value reached the desired value, the culture was incubated on ice for 15 minutes and then centrifuged at 3000 rpm 4°C for 15 minutes. The pellet was resuspended in 33 mL of ice-cold RF1 buffer (**Table *3.1***) and incubated on ice for another 15 minutes. After centrifugation under the same conditions as the previous step, the pellet was resuspended in 8 mL of ice-cold RF2 buffer (***Table 3.2***) and incubated on ice for 15 minutes. As a last step, the suspension in RF2 buffer was aliquoted into 50 or 100 µl aliquots in 1.5 ml microcentrifuge tubes and snap-frozen using liquid nitrogen and stored at -80°C.

Table 3.1 Components of RF1 Buffer Solution. pH value was adjusted to 5.8 with 0.2 M acetic acid.

RF1 Buffer

Reagent	Amount	Final Concentration
RbCl	1.2 g	100 mM
CH_3CO_2K	0.3 g	30 mM
$MnCl_2.4H_2O$	0.99 g	50 mM
Glycerol	12 mL	15% (w/v)
$CaCl_2$	0.15 g	10 mM
dH_2O	up to 100 mL	-

Table 3.2 Components of RF2 Buffer Solution. pH value was adjusted to 5.8 with 0.2 M acetic acid.

RF2 Buffer

Reagent	Amount	Final Concentration
$RbCl_2$	0.06 g	10 mM
$CaCl_2$	0.6 g	75 mM
MOPS	0.11 g	10 mM
Glycerol	6 mL	15% (w/v)
dH_2O	up to 50 mL	-

3.1.4 Bacterial Transformation

50 ng of plasmid was added to chemically competent Stbl3 E. coli strain bacterial suspensions, which had been thawed on ice 5 minutes before. The mixture was incubated on ice for 30 minutes, heat-shocked at 42℃ for 30 seconds, and immediately placed on ice for 5 minutes. 250 µL Super Optimal Broth with Catabolite Repression Medium (SOC) was added to this bacterial suspension mixture and incubated at 37 ℃, 225 rpm for 1 hour with a shaker. After this time, to increase transformation efficiency, the mixtures were centrifuged at the lowest value of centrifuge for 3-5 minutes, the 200 µL supernatant was discarded, and the pellets were resuspended with the remaining 100 µL.

All this 100 µL mixture was spread onto LB agar plates containing either ampicillin or kanamycin and plates depending on the antibiotic resistance gene of the plasmid. Plates were incubated at 37℃ for 16 -18 hours.

3.1.5 Plasmid DNA Purification and Diagnostic Digestions

Firstly, single colonies were picked from each LB-agar plate. Picked colonies inoculated in the required amount of antibiotic-supplemented LB broth (5 mL for Mini prep protocol and 200 mL for Midi Prep protocol.) The tubes, including these bacterial inoculations, were incubated overnight with a shaker at 37 ℃, 225 rpm. Approximately 16-18 hours later, tubes were centrifuged at 3750 rpm, 4℃, for 15 minutes. NucleoSpin Plasmid mini kit (Macherey-Nagel, MN 740588.50) and NucleoBond Xtra midi kit (Macherey-Nagel, MN 740410.10) were used to isolate plasmid DNAs from those precipitated bacteria, and kit protocol instructions were followed with one difference; to obtain more efficient eluted DNAs, at the elution step the tubes incubated at 70℃ instead of Room Temperature (RT) for 2 minutes using with a preheated Elution Buffer at 70℃. Then, each eluted plasmid DNA concentration was measured using a NanoDrop spectrophotometer.

Diagnostic digestion reactions (**Table *3.3***) were set to validate the plasmids by making calculations at the following step of NanoDrop measurement. 1000 ng of plasmid DNA, XhoI, and HindIII enzymes with proper Buffer were added into PCR tubes, and the reaction was carried out at 37℃ for 2 hours on a Thermal Cyler (Bio-Rad- T100). Digested DNA samples were visualized using Gel Doc XR+ Documentation System (Bio-Rad) after running on 1% agarose gel. When the expected bands were confirmed in this way (

Appendix A Figure), continued with the relevant DNA samples for further experimental stages.

Table 3.3: Double Digestion Reaction of pOMGP-TM-GFP or pEGFP-N1 Plasmids by HINDIII and XHOI

Reagent	Volume In 1x Reaction
Buffer 2.1	5 µl
DNA	1 µg
XHOI	1.0 µl (20 Units) †
HINDIII	1.0 µl (20 Units) †
Nuclease Free Water	Up To 50 µl

3.2 Cell Culture

3.2.1 HEK293 and HeLa Cell Culture

HEK293 cells or HeLa cells are both were cultured in the same conditions: at 37 ℃ with 5% CO_2 using Complete DMEM Medium, also called D10 Media, which prepared with high glucose-Dulbecco's Eagle Medium (DMEM) 1X (Sigma, D6429), supplemented with 10% Fetal Bovine Serum (FBS) (Biowest, S181H), and 1% Penicillin/Streptomycin. (Biowest, L0022). When cells reached at least 70% or 80% confluency, they were passaged using Trypsin (Multicell, 325-542-EL) at ratios between 1:6 and 1:10 or frozen using a 10% DMSO-FBS supplemented Freezing Medium.

3.2.2 Transfection Optimizations

Preliminary optimization experiments, well described in "*Section 3.3.1*", were performed using FuGENE®-HD (Promega, E2311). Precisely 24 hours after the transfections', removed cells were collected using FACS Buffer (1% BSA or 1%FBS in 1x PBS) containing Propodium iodide (PI). GFP ratios were measured in Flow Cytometry (Attune NxT, Invitrogen, Thermo Scientific.).

3.3 Optimization of Live Cell Based Assay

For (i.) the first stage of the assay that regarding "culturing and transfection of cells" step, cell type and count, method of removing cells from the plate, DNA concentration and the FuGENE-HD ratio according to the DNA concentration, (ii.) the second stage, named "staining" step, a dilution factor for both 22H6, the primary antibody to detect anti-OMGp antibodies, and Alexa Fluor 647-conjugated Streptavidin used to detect biotin and (iii.) the final stage, related "measurement " step, the “voltage settings” required for measurement have been investigated, respectively.

3.3.1 Culturing and Transfection of Cells

a) Cell type: Optimizations were performed simultaneously in two different cell lines, HeLa and HEK293 cells.

b) Count of cell seeded: Three cell densities, 40.000, 50.000, and 75.000, were utilized per well separately in 24-well plates during transfection experiments.

c) To remove cells from plates: The transfected cells, either with pOMGp-TM-GFP or pEGFP-N1, detached using different removal methods such as Trypsin (37℃ / 5 minutes), ice-cold PBS (at RT / 10 minutes, then on ice / 10 minutes), and ice-cold PBS+ scraper (at RT / 10 minutes).

d) DNA concentration & FuGENE-HD ratio: Trials were conducted with DNA concentrations of 0.75 µg and 1 µg and a DNA: FuGENE ratio between 1.5-4 (including 1.5 and 4). The DNA concentration was scaled to 0.75 µg and 1 µg according to the count of cells used (**Table *3.4***).

Table 3.4 Scaling DNA concentration up/down to 0.75 µg or 1 µg, assuming a starting cell count of 200.000.

Cell Count	**DNA concentrations**	
Per/well	According to **0.75 µg**	According to **1 µg**
40.000	0.15 µg	0.2 µg
50.000	0.19 µg	0.25 µg
75.000	0.28 µg	0.38 µg

3.3.2 Staining

Three dilution factors, 1:1000, 1:2000, and 1:4000, were experimented with for Alexa Fluor 647-conjugated Streptavidin to detect anti-human-IgG-biotin during staining protocol for L-CBA while two different ratios ,1:100 and 1:200, for the primary antibody 22H6, used in the positive control experiments.

3.3.3 Measurement

The assay protocol was applied to cells transfected with pOMGp-TM-GFP or pEGFP-N1; however, cells were incubated with 22H6, the positive control antibody, instead of patient serum or CSF samples. Then, measurements were made in flow cytometry at the two different settings (No:1 and No:2) specified in the

***Table* 3.5.**

Table 3.5 Voltage settings for flow cytometry measurement by the Attune NxT device. The first values tried are NO:1, on the left, and the second is NO:2, on the right.

NO:1	**FSC**	**SSC**	**BL1**	**RL1**	**VL1**	**YL1**	**NO:2**	**FSC**	**SSC**	**BL1**	**RL1**	**VL1**	**YL1**
	A, H, W	A, H, W	**GFP-FITCH**	**OMGP-AF47**		PI		A, H, W	A, H, W	**GFP-FITCH**	**OMGP-AF47**		PI

80	280	**250**	**350**	260	300	80	280	**220**	**300**	260	300

3.4 Live Cell Based Assay

After the optimizations were concluded, the assay steps were performed in the following order and manner.

3.4.1 Sample Prepar*ation*

Patient samples that arrived us from the Neurology clinics of 4 different centers *(Koç University Hospital, Bakırköy Prof. Dr. Mazhar Osman Mental Health and Neurological Diseases Training and Research Hospital, Sakarya Training and Research Hospital, and Hacettepe University Faculty of Medicine)* were included in this study. When the incoming samples were serum or CSF, they were diluted at 1:50 for serum and 1:1 for CSF in the FACS Buffer and used directly in this way. However, if it was in the form of blood, they were centrifuged at 2000 g for 15 minutes to separate serum from blood and used the same as above. All samples were stored in -80°C- refrigerators.

3.4.2 Cell Seed and Transfection

1.425.000 HeLa cells were seeded to 10-cm dishes the day before transfection, then pOMGP-TM-GFP and pEGFP-N1 as control were transiently transfected. For transfection, briefly, 16.03 µl of FuGENE-HD reagent was diluted in 483.97 µl OptiMEM (Gibco, 31985-062) media and mixed with 5.34 µg of plasmid DNA (either pOMGP-TM-GFP or pEGFP-N1) -OptiMEM mixtures, then incubated at RT for 30 minutes. Following the incubation, the whole mixture was slowly and dropwise applied to HeLa cells.

3.4.3 Antibody Staining

Cells were detached from the dishes using Trypsin after 24-hour transfection and seeded as 5 x 10^4 cells per/well in a 96-well plate. Then, the diluted patient's serums were added to those transfected cells and incubated on a shaker in the cold room for 45 min. After washing three times to get rid of serum residues, cells were first incubated with FACS buffer, including goat anti-human-IgG-biotin (Jackson, 109-066-098) at 1:500

ratio in a cold room, on ice with shaking for 30 minutes and secondly, after washing three times, within FACS-buffer including Alexa Fluor 647-conjugated streptavidin (Jackson, 016-600-084) at 1:2000 ratio in dark and the same conditions. After the last incubation, cells were rewashed three times and collected with FACS Buffer, including 1:2000 diluted PI (Sigma, P4170).

3.4.4 Flow Cytometry Measurement

The antibody bindings were analyzed using Flow Cytometry. Before starting the readings, the voltage values given below ***(*** **Table *3.6)*** were set on the device, and 20.000 events were recorded in each measuring. pEGFP-N1 transfected cells were used as a control for gating.

Table 3.6 The Optimized Voltage Settings for Attune NxT.

FSC	SSC	BL1	RL1	VL1	YL1
A, H, W	A, H, W	GFP	OMGP		PI
80	280	220	300	260	300

3.5 Isotype Testing

For detecting isotypes of OMGp antibody in positive patients, an isotype test was conducted just as described in the Live Cell-Based Assay section but with one modification. The secondary anti-human-IgG antibody was replaced by a 1:100 dilution of anti-human-IgG1, anti-human-IgG2 or anti-human-IgG3, 1:500 dilution of anti-human-IgG4 and 1:100 dilution of IgM respectively. In addition, the test was repeated using a more concentrated dilution factor, such as 1:10 or 1:20 dilution of these antibodies. The antibodies used in subtyping experiments listed in **Table *3.7*** .

Table 3.7 Antibodies used in isotyping experiments.

Antibodies	Source	Catalog No	Working Concentration
Anti-Human-IgG1-Fc-BIMA (clone: HP6001)	Mouse	Southern Biotech, 9054-28	1:100 or 1:10
Anti-Human-IgG2-Fc-BIOT (clone: HP6002)	Mouse	Southern Biotech, 9070-08	1:100 or 1:20
Anti-Human-IgG3-Hinge-BIOT (clone: HP6050)	Mouse	Southern Biotech, 49210-08	1:100 or 1:20
Anti-Human-IgG4-Fc-BIOT (clone: HP6025)	Mouse	Southern Biotech, 9200-08	1:500 or 1:20
Anti-Human IgM Monoclonal Antibody (clone: SA-DA4), Biotin	Mouse	Invitrogen, 13-9998-82	1:100 only

3.6 Statistical Analysis

3.6.1 Delta MFI and MFI Ratio Calculation

Data obtained from flow cytometry measurements were quantified through FlowJo v10 software and Microsoft Excel. Firstly, dead cells with positive propidium iodide staining were excluded. Then, fluorescence intensity was determined by gating on the highly EGFP-positive live cells with fluorescence intensity >500. Finally, the mean fluorescence intensity (MFI) ratio (**Equation *1***) and the Delta MFI (Δ MFI) (**Equation *2***) of the reactivity to pOMGP-TM-EGFP and EGFP alone values were calculated using the formulas below.

Equation 1: Calculation of MFI Ratio

$$MFI\ Ratio = MFI\ \frac{pOMGP}{eGFP}$$

Equation 2 : Calculation of Δ MFI

$$\Delta \text{ MFI} = MFI(pOMGP) - MFI(eGFP)$$

3.6.2 Cut- off Value Determination

The threshold was determined by scanning the sera of all 30 individuals of the healthy control group for anti-OMGp antibodies through CBAs performed at different times. Δ MFI and MFI ratios were calculated for each healthy individual using the geometric means obtained from these scans. The average for Δ MFI and MFI Ratio was taken separately, and standard deviations (SD), "Mean + 3SD", "Mean + 4SD", "Mean + 5SD", and "Mean + 6SD", were calculated (**Table *3.8***). Thereby, strict cut-off values were decided for both Δ MFI and MFI Ratio.

Table 3.8 Cut-off Value Determination

Mean+ X SDs	Δ MFI	MFI Ratio
X=3	27.8	1.2
X=4	45.9	1.3
X=5	64.1	1.4
X=6	82.3	1.5

3.6.3 Data Analysis

Graphs were generated using Prism v8.0a (GraphPad Software) and bioicons.com

Chapter 4:
RESULTS

4.1 A Live Cell Based Assay Optimized to Detect Anti-OMGp Antibodies

4.1.1 Outcomes of Transfection Optimization

Twenty-four hours after the transfection, which was accomplished in the plate outline schematically shown in **Figure *4.1***, the GFP ratios of the cells were measured by flow cytometry, and the values shown in ***Table 4.1*** and ***Table 4.2*** were obtained.

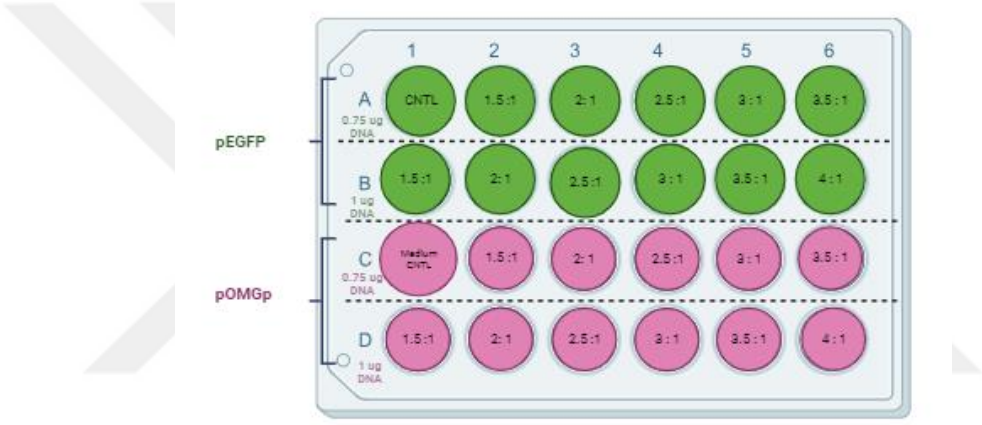

Figure 4.1 The plate outline used at three different cell densities. The plate outline was used at three cell densities, 40.000, 50.000, or 75.000 cells in each well. The wells' numbers show the FUGENE: DNA ratio used for the indicated well.

Table 4.1 GFP transfection percentage rates obtained by flow cytometry in HeLa cells transfected with pOMGp-TM-GFP and pEGFP-N1. Well number: A1:1 for pEGFP-N1; A2:2; A3:3…. B1:7, B2:8, B3:9; C1:1 for pOMGp1; C2:2; C3:3…. it progresses as D1:7, D2:8, D3:9. Values above 50% are highlighted in the table. red indicates 40,000 cells/well plate, orange indicates 50,000 cells/well plate, and yellow indicates 75,000 cells/well plate.

	GFP RATIOS IN %			POMGP-TM-GFP RATIOS IN %		
Well No:	Cell Count / Well:					
	40K	50K	75K	40K	50K	75K
1 (CNTL)	0.13	0.16	0.089	0.13	0.47	0.15
2	40.9	40.2	8.13	38.2	33.7	1.36
3	12.9	**53.5**	19.6	**54.0**	45.1	24.8
4	**50.9**	**52.5**	42.7	**57.2**	**50.9**	20.0
5	**55.9**	**55.3**	48.3	**58.8**	**56.3**	45.8
6	**54.8**	**61.4**	45.7	**61.6**	**54.8**	**54.6**
7	45.8	31.3	25.2	46.9	13.3	13.4
8	39.4	33.2	19.5	40.5	**58.1**	19.2
9	**54.9**	44.5	30.8	**64.5**	47.7	44.9
10	**53.3**	**50.1**	45.1	**61.3**	**55.6**	**54.0**
11	**53.2**	**52.9**	42.7	**60.1**	**56.0**	**55.1**
12	**55.3**	**61.6**	47.8	**57.2**	**56.8**	49.9

Table 4.2 GFP transfection percentage rates obtained by flow cytometry in HEK293 cells transfected with pOMGp-TM-GFP and pEGFP-N1. Well number: A1:1 for pEGFP-N1; A2:2; A3:3…. B1:7, B2:8, B3:9; C1:1 for pOMGp1; C2:2; C3:3…. it progresses as D1:7, D2:8, D3:9. Values above 50% are highlighted in the table. Red indicates 40,000 cells/well plate, orange indicates 50,000 cells/well plate, and yellow indicates 75,000 cells/well plate.

	GFP RATIOS IN %			POMGP-TM-GFP RATIOS IN %		
Well No:	Cell Count/ Well:					
	40K	50K	75K	40K	50K	75K
1 (CNTL)	0.021	0.033	0.011	0.037	0.091	0.037
2	**67.4**	46.5	29.5	18.2	24.2	15.4
3	**60.6**	47.2	41.7	35.3	31.3	18.3
4	**67.6**	45.6	31.1	47.5	38.5	41.2
5	**60.2**	**60.1**	**50.6**	**59.5**	35.8	37.9
6	**69.5**	**54.1**	**56.5**	**64.3**	**52.0**	**54.9**
7	37.3	17.7	11.2	3.43	1.15	2.63
8	46.9	32.4	33.6	21.6	32.5	24.3
9	**61.9**	**50.4**	**50.8**	**62.8**	43.9	43.4
10	**60.7**	45.1	**63.8**	**59.4**	24.9	**50.7**
11	**64.3**	**63.6**	47.7	**66.7**	48.2	**53.9**
12	**67.8**	**66.8**	**57.2**	**67.5**	**68.7**	**58.9**

In line with these results, it was decided to proceed with HeLa cells (**Table *4.3***) and cell detachment methods were tried on these cells; the values in the **Table *4.4*** were obtained.

Table 4.3 HeLa cell density and FUGENE:DNA ratios decided by GFP ratio

GFP Ratio	Cell Density	FUGENE: DNA Ratio

55.3% for pEGFP-N1 transfected cells & **56.3%** for pOMGp-TM-GFP transfected cells	50.000 per well	3:1

Table 4.4 Results of the experiment for different detachment methods. MFI values and transfection rates acquired from flow cytometry measurements after cells transfected with pOMGp-TM-GFP or pEGFP-N1 were removed from the plates by different detachment methods.

Method	Delta MFI	MFI Ratio	GFP Ratio	pOMGp-TM-GFP Oranı
Trypsine	30,2	1,42	43.02%	39.35%
Ice Cold PBS	57,1	1,64	41.76%	39.19%
Ice cold PBS+scraper	55,2	1,60	41.6%	38.61%

4.1.2 Optimization of Staining

Different dilution factors as 1:1000, 1:2000, and 1:4000 was tested for Alexa Fluor 647-conjugated Streptavidin to detect anti-human-IgG-biotin, used in the staining protocol following the incubation of cells transfected with pOMGp-TM-GFP and pEGFP-N1 plasmids as control with patient serum and CSF samples. In accordance with the data obtained (***Table 4.5*** and **Appendix A Figure**) 1:2000 ratio was picked.

Table 4.5 Optimization results of Alexa Fluor 647-conjugated Streptavidin antibody. MFI values of cells transfected with pOMGp-TM-GFP or pEGFP-N1 in which dilution factors were tested of Alexa Fluor 647-conjugated Streptavidin 1:4000, 1:2000, and 1:1000.

Dilution Factor	Delta MFI	MFI Ratio
1:4000	512	3.34
1:2000	**846**	**5.23**
1:1000	994	5.78

The optimization studies were also carried out at two different rates,1:100 and 1:200, for the primary antibody 22H6 used as a positive control and the ratio 1:200 was chosen based on data given at ***Table 4.6*** *and*

Appendix A Figure 2.

Table 4.6 22H6 positive control antibody optimization outputs. MFI values of cells transfected with pOMGp-TM-GFP or pEGFP-N1 in which dilution factors were tested of 22H6 positive control antibody 1:100 and 1:200.

Dilution Factor	Delta MFI	MFI Ratio
1:100	7248	61.4
1:200	**6947.4**	**72.2**

4.1.3 Voltage settings that give the best measurement

For voltage settings, two different options provided values in the (**Table *3.5***)were attempted and the graph given in the **Figure *4.2*** was gained.

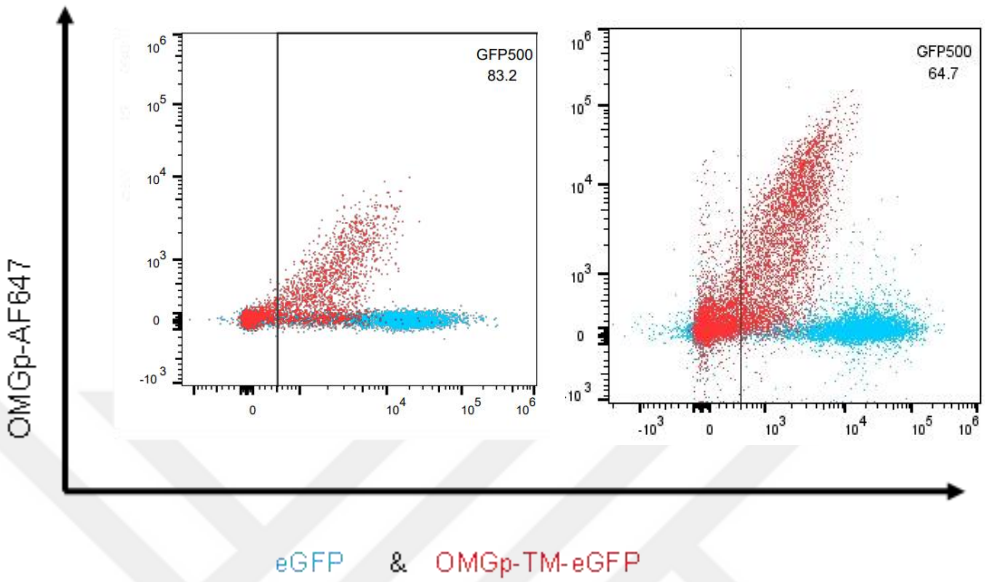

Figure 4.2 Quantification of pOMGp-TM-GFP & pEGFP transfected cells incubated with 22H6 antibody then measured by flow cytometry at different voltage settings. 22H6 positive control antibody dilution 1:200, measurement no:1 voltage setting on the left; measurement no:2 voltage setting on the right.

4.2 The Features of Study Cohort

834 patients, aged between 16 and 90, with a gender distribution of Female: Male =xx from the Neurology clinics of 4 different centers *(Koç University Hospital, Bakırköy Prof. Dr. Mazhar Osman Mental Health and Neurological Diseases Training and Research Hospital, Sakarya Training and Research Hospital, and Hacettepe University Faculty of Medicine, respectively.)* were included in the study. The serum of these 834 patients with the CSF of 86 patients from that population was scanned with the developed CBA assay. For the serum cohort, while …% of these 834 individuals are MS patients, this was followed by the IDD group with…% so closely. The rest of the cohort comprised % NMOSD, % MOGAD, and % OND **Table *4.7***.

Table 4.7 Primary characteristics of the patient cohort whose serum was studied.

Cohort	Number	Average Age	Female	Male
IDD	182	44	126	56
MS/CIS	187	37	123	64
NMOSD	32	45	24	8
MOGAD	38	43	3	35
OND	103	47	52	51
HC	30	44	12	18
TOTAL: (patient)	542	43	328	214

When the clinical characteristics of the patients in the CSF cohort were examined, individuals were placed in three primary classes with 46.5 % IDD, 30.2 % MS, and 23.3% OND (**Table *4.8***).

Table 4.8 Primary characteristics of the patient cohort whose CSF was studied.

Cohort	Number	Average Age	Female	Male
IDD	40	43	25	15
MS/CIS	26	36	17	9
OND	20	44	11	9
TOTAL:	86	41	53	33

4.3 Anti-OMGP Could Be Found in Serum but not in CSF.

4.3.1 The Criteria to Called an " Anti-OMGP Positive Patient"

Three primary criteria were determined to evaluate the data obtained from the scanned patient serum and CSF samples as positive or negative for OMGp autoantibodies: (i.) Delta MFI value should be ≥ 110, (ii.) MFI Ratio should be ≥ 1.7, and (iii.) As can be

seen in **Figure *4.3*** , a distinct peak observed in the graphs acquired from flow cytometry. The L-CBA test was repeated thrice with patient sera that met all three criteria. Patients who continued fulfilling the criteria in all replications were classified as positive, while the rest were defined as negative.

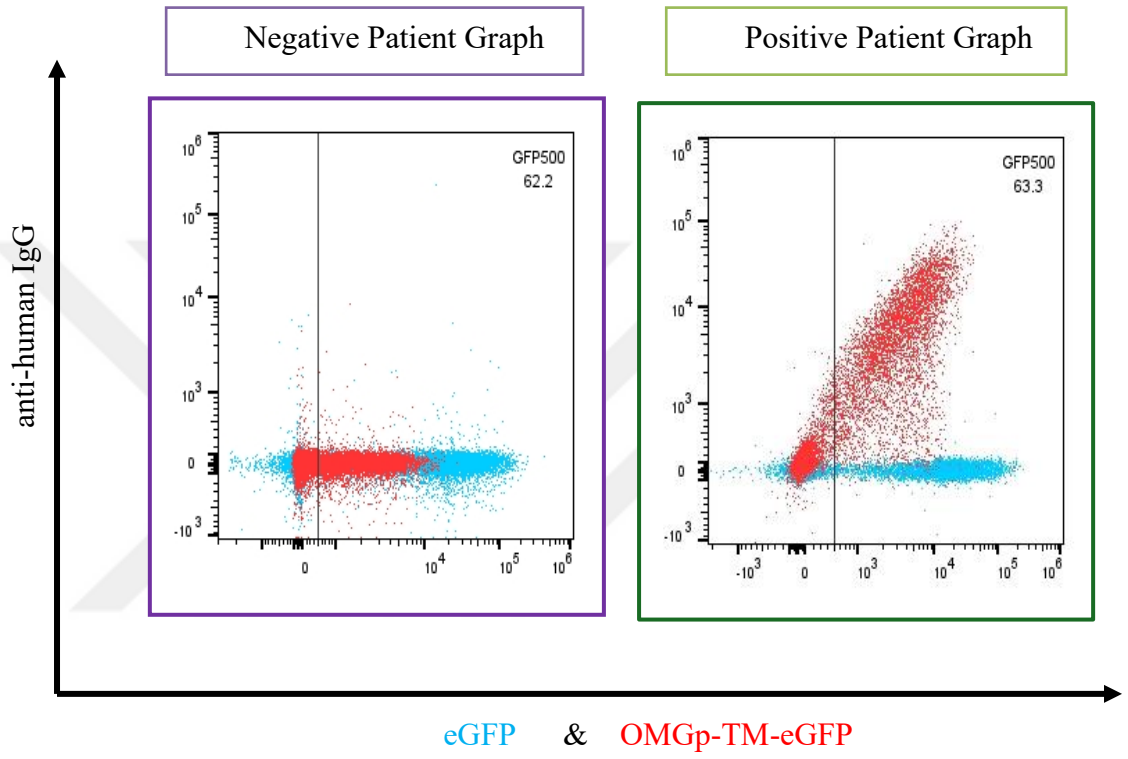

Figure 3 Sample of negative and positive patient graphs. The data were obtained from Flow cytometry measurements.

4.3.2 Anti-OMGP Positive Patients

In accordance with the determined criteria above, net positivity was detected in the sera of 17 patients (**FIGURE**), whereas all CSF samples were negative. All patients with positive anti-OMGp antibodies have negative MOG and AQP4 antibodies. None have a typical

MS diagnosis: instead, they had atypical demyelinating disease features. The mean age of positive cases is ... (range XX-YY), and the female: male ratio is A (**Table *4.9***).

Table 4.9 Primary characteristics of the anti-OMGp positive patients

Cohort	Number	Average Age	Female	Male
Positive patients	17			

4.4 Autoantibodies Targeting anti-OMGP in Patients with Atypical Demyelinating Diseases

In case the clinical features of the 17 positive cases were examined in more detail, it was seen that they mostly have atypical demyelinating characteristics, which enclosed tumefactive lesions (in four patients), ADEM-like lesions (in three patients), long segment transverse myelitis (in two patients) and cortical lesion (one patient). The OCB was positive in 33.3% of patients. From a diagnostic perspective, eight of the patients have atypical demyelinating disease diagnoses, whereas one has autoimmune encephalitis. PLEX was required in one of the patients during the attack, which responded well. In three patients diagnosed with atypical MS and treated with betaferon or glatiramer acetate, upper-line treatment was started as the attacks continued, but the relapses persisted under therapy. All these clinical aspects of these patients are summarized in ***Table 4.10*** .

Despite the table above providing detailed clinical data about the cases, we detected positive, examining a few cases selected from the table will be useful to understand better the course of the disease and the extent of the treatment options applied.

Case 1: The patient had a first attack at the age of 16. In the beginning, he had acute myelitis involving the entire cord, and OCB was negative. So, steroid treatment was started, but three days later, he developed a tumefactive lesion in the left hemisphere while under steroid treatment. PLEX + IVIG treatment was started, and the patient's recovery was observed. When the patient was 22 years old, he had his second attack. This time, he had tumefactive and ADEM-like lesions in the right hemisphere and brainstem, very similar to those six years ago. Although steroid treatment was tried again, the patient's response to steroids was feeble, and it seemed that he had recovered through PLEX again.

Case 2: Although the patient, whose age at onset was 17, was under treatment Rebif between 2013 and 2020, she had five attacks during remedy. OCB was negative in 2013 and positive, with a low IgGi score in 2020. Between 2020 and 2024, her treatment was updated with Ocrelizumab; from this point, she did not have an attack.

Case 3: This patient applied to the clinic with complaints of ataxia, vertigo, loss of strength, and sensation on the left, and had her first attack in February 2021. She had one cortical, contrast-enhancing lesion on MRI, as well as lesions in the bulbus and middle cerebellar peduncle. The patient, who started steroid treatment, had her second attack five months later while under remedy, and came to the clinic complaining of vision loss. This time, her MRI showed hyperintensity in the left optic nerve, extending to the optic chiasm. Therefore, AZA was started as a treatment, and it seems she did not have a re-attack.

Case 4: This 62-year-old female patient, who employed to the clinic with complaints of dysarthric speech and ataxic gait, had diffuse hyperintense lesions in the pons and middle cerebellar peduncle on MRI.

4.5 The IgG3 Isotype identified in Only One Patient

IgG3 subtype was detected at high levels in only one net-positive patient, while the rest were negative for all isotypes **(FIGURE)**. Furthermore, other subtypes, IgG1, IgG2, and IgG4, were not found in that IgG3-positive patient. When the experiment was repeated with more concentrated antibody dilutions, no isotype was encountered other than the IgG3 isotype identified in a same single patient again. In addition, no positivity was noticed in the IgM isotyping study accompanied by healthy controls. As a note, a control pilot study was carried out on the functioning of the antibodies with positive controls, and no trouble was detected ***(Appendix A Figure 4).***

Table 4.10 Clinical Features of anti-OMGp-IgG Positive Patients. The relevant table was formed based on the clinical knowledge available to us. "+"; if the corresponding feature is positive in the patient; and "-" if it is negative. Those without information are left blank. ADD, Atypical Demyelinating Diseases; ADEM, acute disseminated encephalomyelitis; ON, Optic Neuritis; LETM, longitudinally extensive transverse myelitis; OCB, oligoclonal bands; MS, multiple sclerosis; RRMS, relapsing-remitting MS; AZA, azathioprine; OCZ, ocrelizumab; IVMP, intravenous methylprednisolone pulse; IVIg + PE; intravenous immunoglobulin + plasma exchange.

Diagnosis	Onset Age	Attacks Number	Cortical Lesions	Tumefactive Lesions	ADEM-like Lesions	BrainstemLesions	Lesion Resolution	ON	LETM	OCB	Treatment Response
ADD	53	2	+	–	–	+	+	–	+	–	2nd attack under steroids; No attacks after AZA
Tumefactive MS	36	2+	–	+	–	–	+	–	–	+	GA inadequate OCZ useful
Tumefactive MS	18	2	–	+	+	+	+	–	–	In 2013: - In 2020: +	5 attacks under Rebif; No attacks after OCZ;
Isolated Brainstem Demyelinating Disease	59	1	–	–	–	+	–	–	–	–	limited response to IVMP
ADEM-MS with Tumefactive Lesion	17	2		+	+	+	+	–		–	Attacks under Rebif
RRMS (single attack)	57	1	–	–	–	+	–	–	–		
Atypical MS (LETM onset)	32		–	–	–		–	+		+	

mADEM with Tumefactive Lesion	16	2	+	+	+	+	+	+	–	–	Steroids are insufficient, improvement with IVIg + PE
Autoimmune Encephalitis	53	1				–	+	–			
A1											
A2											
A3											
A4											
A5											
A6											
A7											

Chapter 5:
DISCUSSION

Within the scope of this thesis, firstly, the high-throughput L-CBA, general flow of is given in **Figure *2.9***, was established to detect possible anti-OMGp autoantibodies in patient serum and CSF samples for the first time in Turkey. To achieve this, firstly, the pEGFP-N1plasmid DNA, used for control purposes, and pOMGp-TM-GFP, which reached us embedded in the filter paper from our collaboration, were eluted from the filter paper and amplified. Then, diagnostic digestion was carried out using appropriate restriction enzymes. Thus, the obtained plasmids were verified (

Appendix A Figure 1) and optimization experiments were carried out to determine superior and the most efficient values for the assay.

HeLa and HEK293 cell lines were preferred during optimization experiments to having the highest transfectability. The cell counts to seed was determined by considering Thermo Fisher Scientific's recommended rates ((TFS), 2024) for the amounts to be seeded according to the m^2 calculation and the seed amount recommended by ATCC based on cell type (ATCC, 2024). In this direction, cell counts were scaled up according to 24-well plate dimensions, which were favoured during optimizations, and simultaneously seeded at the 40.000,50.000 and 75.000 densities separately. The cell lines were then transfected using the FuGENE-HD chemical because it minimizes toxicity and is generally easy to optimize for the best results. Since FuGENE-HD was used during transfection, the usage dose of DNA concentrations and the chemical ratio based on those concentrations throughout optimizations were determined in line with the values Promega recommended (Promega, 2024).

Although high amounts of GFP were obtained in both cell lines at different densities or DNA concentrations (**Table *4.1*** and **Table *4.2***), HeLa cells were chosen for further experiments with a 50.000 cell density and a FUGENE: DNA ratio of 3:1 because the most consistent GFP ratio values between the control group and pOMGp-TM-GFP-transfected cells were obtained in this cell line and ratios. (**Table *4.1*** and **Table *4.3***.). Before scanning patient serum and CSF samples via optimized L-CBA, the transfected HeLa cells were also investigated using three distinct detachment methods to determine whether they were chemically affected by the removal method and impacted the result obtained from the measurement method. However, utilizing trypsin, which is the common

and easy method used to remove HeLa cells, was continued as no significant difference was detected between control methods. Thus, the cell type and cell count for culturing, detachment method, and transfection procedure to express the relevant plasmids in the cell were determined, and the most prominent values were chosen for the assay's initial stage and proceeded with optimizations for the next one.

After incubation with patient serum or CSF samples, the transfected cells are exposed to a series of staining procedures to identify the existence of potential autoantibodies in these samples during this step. Pinpointing the proper working concentration of the antibodies or fluorescent conjugates used to catch antibodies is extremely important. Because, for instance, a much-concentrated dilution factor chosen as the working concentration may cause background signals during flow cytometry measurements since the intensity or level of fluorescence are detected. In contrast, lower dilution factors are insufficient to detect possible antibodies. Considering this situation, a dilution factor determination study was carried out for the antibodies and fluorescence conjugates, which were employed for the first time in the assay. If the outputs between the more diluted and concentrated versions were similar, diluted values were used to avoid possible background noise for the flow cytometry measurements.

Flow cytometry measurements are used to quantify and visualize the resulting data after all staining procedures are completed to specify the level of autoantibody binding. Microscopy was also often preferred for this purpose. In fact, the most commonly utilized “read-out” after immunocytochemistry had been confocal microscopy analysis (Amatoury et al., 2013). However, microscopy live cell-based assays are semi-quantitative and observer-dependent, whereas flow cytometry is an observer-independent, accurate, and reliable detection method (P. J. Waters et al., 2012). Flow cytometry cell-based assays have also been shown (Pröbstel et al., 2011; Reindl et al., 2020) to successfully detect autoantibodies in patients with demyelinating diseases, which made this method more beneficial for our study. Thereby, employing flow cytometry cell-based assay is advantageous as it allows quantitative assessment of serum binding to antigen-expressing cells and control cells in a short time with validated (P. J. Waters et al., 2019; Yeh & Nakashima, 2019) high sensitivity and specificity.

In order to proceed with this technique, it is first necessary to determine the device's fitting voltage settings. Here, measurements were performed under two different settings to decide the proper voltage settings (**Table *3.5***). Since a more distinct peak value was

captured in the measurements made during the No:2 voltage setting (**Table *3.6*** and **Figure *4.2***), this was favored for scanning patient samples. Due to data complexity and possible nonspecific binding in human serum, flow cytometry data received after screening patient specimens must be analyzed and interpreted attentively Although different analyses have been reported, the surest way to compare serum binding to antigen-expressing cells with control cells is by assessing autoantibody titers by subtraction (Δ MFI) or division (binding ratio=MFI ratio) together with using reasonable thresholds (Tea et al., 2020). Since, in some cases, low titer antibodies can be detected somehow in healthy individuals or other neurological controls, it is vital to determine the exact cut-off to increase the diagnostic specificity for the antibody of interest.

Therefore, we calculated Δ MFI and MFI ratio values for each patient sample and healthy controls. Subsequently, we established two stringent cut-off values *(Section 4.3.1: 4.3.1 The Criteria to Called an " Anti-OMGP Positive Patient")* by calculating the "mean+ SD" values of Δ MFI and MFI Ratios of health controls separately to interpret these values and avoid false positive or negative results by increasing further diagnostic specificity. Accordingly, we evaluated each patient's results coming from the assay. If the Delta MFI and MFI ratio calculated for each patient were above both cut-off values in all three repeats, along with the graphs showing a distinct peak, we assumed the patient was positive. In continuation, isotyping experiments were performed with IgG1, IgG2, IgG3, and IgG4 antibodies as two-replicate to determine the predominant IgG isotype for anti-OMGp in those patients detected positive. Although we expected to find a largely IgG1 isotype for anti-OMGP-Abs, like anti-MOG (Winklmeier et al., 2019) or anti-AQP4(P. J. Waters et al., 2012), this isotype was not found in our positive patients. Instead, interestingly, the IgG3 was detected in only one net positive patient, whereas other isotypes were negative. In contrast, the remaining patients were negative for all isotypes, suggesting that it may be due to the clinical characteristics of those patients or timeline of disease occur.

Patients scanned with our optimized anti-OMGp specific L-CBA were basically classified into five groups, IDD, MS/CIS, NMOSD, MOGAD, and OND, based on their clinical diagnosis. Most of the MS/CIS group patients were typical MS patients. However, some patients showed atypical features such as tumefactive MS and were conflicted in their diagnosis but still included in this group. Alongside this, most patients with NMOSD and MOGAD meet the diagnostic criteria for their disease, but still, there

were some atypical ones. If patients have not been definitively diagnosed due to their discriminative atypical features but are known to have autoimmune demyelinating disorders, then they were classified under the IDD group and patients without demyelinating disorders but still have atypical features were added in the OND group. Thus, anti-OMGP autoantibodies were tested and detected in a study cohort that was very rich in terms of atypical features.

When the clinical and radiological characteristics of those anti-OMGP positive patients were examined in detail, atypical demyelinating features such as tumefactive lesions, widespread ADEM-like lesions, LETM, and cortical lesions (**Table 4.10**) were seen in the patients, supporting our hypothesis firmly. These patients were who did not respond to typical steroid treatment and required other treatment options, such as PLEX and IVIg, which are treatments generally associated with atypical diseases, or maintenance treatments, such as ocrelizumab. Regarding their clinical diagnoses, the fact that X/17 patients were in the IDD group and A/17 were in the MS group, but Y/A showing distinct atypical features stresses the point from which our hypothesis stemmed clearly. In other words, anti-OMGp autoantibody identification in patients from the IDD group, which constituted much of our study cohort, indicates that one of the unknown autoimmune target antigens of atypical demyelinating diseases may be the OMGp protein. Moreover, positive anti-OMGp autoantibody cases (2 out of 10 patients) detected in the only study (Gerhards et al., 2020) on the subject in the literature had atypical features like our findings. Besides, Anti-OMGP autoantibodies detected among patients classified as MS but showed mostly atypical features recalling the emergence of AQP4-IgG (+) NMOSD and MOGAD diseases.

AQP4-IgG+ NMOSD and MOGAD disease patients were being assessed under the name MS due to similar clinical symptoms until these diseases were defined as a separate group(Lennon et al., 2004; O'Connor et al., 2007). Thanks to the development of live cell-based assays, currently known as the gold standard for autoantibody diagnosis, (Mader, Kümpfel, & Meinl, 2020) has allowed the specific identification of MOG-IgG and AQP4 antibodies in relevant diseases and the classification of these diseases as separate disease entities rather than MS. So, our findings in the light of this knowledge were evaluated, it has concluded that anti-OMGp antibodies could cause a separate disease entity as anti-MOG-IgG or anti-AQP4-IgG and should be tested in people with atypical demyelinating disease characteristics.

Taken all together, this would be promising, especially in terms of the recovery process of those patients and have assisted physicians with further diagnosis and treatment more accurately in the early period. However, more comprehensive additional studies with extensive case series are needed to see the further effects of this novel target antigen as a biomarker, build an accurate phenotype characterization, and generate diagnostic and management consensus guidelines for anti-OMGp-IgG-related disorders.

Chapter 6:
CONCLUSION

In this study, the anti-OMGp autoantibodies were tested in a cohort rich in atypical demyelinating diseases for the first time in the literature. Through anti-OMGp-specific live cell-based assay, which we optimized in all aspects and established at our laboratory for the first time in Turkey, 17 clear positive patients were well identified out of 834 scanned patients. All these patients had atypical demyelinating disease features in terms of clinical, radiological, and treatment response and had been classified under IDD or atypical MS predominantly. Considering such diseases classified under IDD or atypical MS, their diagnosis had been challenging us due to their atypical features, which leads to conflict in diagnosis most of the time. However, we now propose in light of our findings that the OMGp protein could be the autoimmune target antigen of patients with atypical demyelinating disorders and cause a distinct disease entity via anti-OMGp autoantibodies. We suppose that these antibodies could be positive in people presenting atypical demyelinating disease characteristics, especially those with large atypical/tumefactive lesions or widespread ADEM-like lesions, and we suggest testing for anti-OMGP antibody positivity in them. In this way, the clinical spectrum of those patients would be understood better, and more reasonable treatment options would be favorable at the earliest time points. Supporting our findings with further retrospective and prospective experimental plans and additional studies is essential to construct consensus regarding anti-OMGp-IgG-related disorders.

BIBLIOGRAPHY

(TFS), T. S. (2024). Useful Numbers for Cell Culture. Retrieved from https://www.thermofisher.com/tr/en/home/references/gibco-cell-culture-basics/cell-culture-protocols/cell-culture-useful-numbers.html

Adams, R. D., & Kubik, C. S. (1952). The morbid anatomy of the demyelinative disease. *Am J Med, 12*(5), 510-546. doi:10.1016/0002-9343(52)90234-9

Amatoury, M., Merheb, V., Langer, J., Wang, X. M., Dale, R. C., & Brilot, F. (2013). High-throughput flow cytometry cell-based assay to detect antibodies to N-methyl-D-aspartate receptor or dopamine-2 receptor in human serum. *J Vis Exp*(81), e50935. doi:10.3791/50935

Armangue, T., Olivé-Cirera, G., Martínez-Hernandez, E., Sepulveda, M., Ruiz-Garcia, R., Muñoz-Batista, M., . . . Dalmau, J. (2020). Associations of paediatric demyelinating and encephalitic syndromes with myelin oligodendrocyte glycoprotein antibodies: a multicentre observational study. *Lancet Neurol, 19*(3), 234-246. doi:10.1016/s1474-4422(19)30488-0

ATCC. (2024). Maintaining Cells. Retrieved from https://www.atcc.org/the-science/culturing-cells/maintaining-cells#:~:text=Depending%20upon%20the%20cell%20type,slowly%2C%20or%20die%20out%20completely.

Banks, S. A., Morris, P. P., Chen, J. J., Pittock, S. J., Sechi, E., Kunchok, A., . . . Flanagan, E. P. (2020). Brainstem and cerebellar involvement in MOG-IgG-associated disorder versus aquaporin-4-IgG and MS. *J Neurol Neurosurg Psychiatry*. doi:10.1136/jnnp-2020-325121

Banwell, B., Bennett, J. L., Marignier, R., Kim, H. J., Brilot, F., Flanagan, E. P., . . . Palace, J. (2023). Diagnosis of myelin oligodendrocyte glycoprotein antibody-associated disease: International MOGAD Panel proposed criteria. *Lancet Neurol, 22*(3), 268-282. doi:10.1016/s1474-4422(22)00431-8

Beh, S. C., Greenberg, B. M., Frohman, T., & Frohman, E. M. (2013). Transverse myelitis. *Neurologic clinics, 31*(1), 79-138.

Bennett, J. L., Costello, F., Chen, J. J., Petzold, A., Biousse, V., Newman, N. J., & Galetta, S. L. (2023). Optic neuritis and autoimmune optic neuropathies: advances in

diagnosis and treatment. *Lancet Neurol, 22*(1), 89-100. doi:10.1016/s1474-4422(22)00187-9

Bhat, A., Naguwa, S., Cheema, G., & Gershwin, M. E. (2010). The epidemiology of transverse myelitis. *Autoimmunity reviews, 9*(5), A395-A399.

Braithwaite, T., Subramanian, A., Petzold, A., Galloway, J., Adderley, N. J., Mollan, S. P., . . . Denniston, A. K. (2020). Trends in Optic Neuritis Incidence and Prevalence in the UK and Association With Systemic and Neurologic Disease. *JAMA Neurol, 77*(12), 1514-1523. doi:10.1001/jamaneurol.2020.3502

Cafferty, W. B., Duffy, P., Huebner, E., & Strittmatter, S. M. (2010). MAG and OMgp synergize with Nogo-A to restrict axonal growth and neurological recovery after spinal cord trauma. *J Neurosci, 30*(20), 6825-6837. doi:10.1523/jneurosci.6239-09.2010

Chang, K. J., Susuki, K., Dours-Zimmermann, M. T., Zimmermann, D. R., & Rasband, M. N. (2010). Oligodendrocyte myelin glycoprotein does not influence node of ranvier structure or assembly. *J Neurosci, 30*(43), 14476-14481. doi:10.1523/jneurosci.1698-10.2010

Cobo-Calvo, A., Ruiz, A., Maillart, E., Audoin, B., Zephir, H., Bourre, B., . . . Marignier, R. (2018). Clinical spectrum and prognostic value of CNS MOG autoimmunity in adults: The MOGADOR study. *Neurology, 90*(21), e1858-e1869. doi:10.1212/wnl.0000000000005560

de Mol, C. L., Wong, Y., van Pelt, E. D., Wokke, B., Siepman, T., Neuteboom, R. F., . . . Hintzen, R. Q. (2020). The clinical spectrum and incidence of anti-MOG-associated acquired demyelinating syndromes in children and adults. *Mult Scler, 26*(7), 806-814. doi:10.1177/1352458519845112

Del Negro, I., Pauletto, G., Verriello, L., Spadea, L., Salati, C., Ius, T., & Zeppieri, M. (2023). Uncovering the Genetics and Physiology behind Optic Neuritis. *Genes (Basel), 14*(12). doi:10.3390/genes14122192

Di Pauli, F., & Berger, T. (2018). Myelin Oligodendrocyte Glycoprotein Antibody-Associated Disorders: Toward a New Spectrum of Inflammatory Demyelinating CNS Disorders? *Front Immunol, 9*, 2753. doi:10.3389/fimmu.2018.02753

Eva, L., Pleș, H., Covache-Busuioc, R. A., Glavan, L. A., Bratu, B. G., Bordeianu, A., . . . Ciurea, A. V. (2023). A Comprehensive Review on Neuroimmunology: Insights

from Multiple Sclerosis to Future Therapeutic Developments. *Biomedicines, 11*(9). doi:10.3390/biomedicines11092489

Ford, H. (2020). Clinical presentation and diagnosis of multiple sclerosis. *Clin Med (Lond), 20*(4), 380-383. doi:10.7861/clinmed.2020-0292

Franklin, R. J., & Ffrench-Constant, C. (2008). Remyelination in the CNS: from biology to therapy. *Nat Rev Neurosci, 9*(11), 839-855. doi:10.1038/nrn2480

Geoffroy, C. G., & Zheng, B. (2014). Myelin-associated inhibitors in axonal growth after CNS injury. *Curr Opin Neurobiol, 27*, 31-38. doi:10.1016/j.conb.2014.02.012

Gerhards, R., Pfeffer, L. K., Lorenz, J., Starost, L., Nowack, L., Thaler, F. S., . . . Meinl, E. (2020). Oligodendrocyte myelin glycoprotein as a novel target for pathogenic autoimmunity in the CNS. *Acta Neuropathol Commun, 8*(1), 207. doi:10.1186/s40478-020-01086-2

Gil, V., Bichler, Z., Lee, J. K., Seira, O., Llorens, F., Bribian, A., . . . Del Río, J. A. (2010). Developmental expression of the oligodendrocyte myelin glycoprotein in the mouse telencephalon. *Cereb Cortex, 20*(8), 1769-1779. doi:10.1093/cercor/bhp246

Greco, G., Colombo, E., Gastaldi, M., Ahmad, L., Tavazzi, E., Bergamaschi, R., & Rigoni, E. (2023). Beyond Myelin Oligodendrocyte Glycoprotein and Aquaporin-4 Antibodies: Alternative Causes of Optic Neuritis. *Int J Mol Sci, 24*(21). doi:10.3390/ijms242115986

Grubisha, M. J., Sun, T., Eisenman, L., Erickson, S. L., Chou, S., Helmer, C. D., . . . Sweet, R. A. (2021). A Kalirin missense mutation enhances dendritic RhoA signaling and leads to regression of cortical dendritic arbors across development. *Proc Natl Acad Sci U S A, 118*(49). doi:10.1073/pnas.2022546118

Habib, A. A., Marton, L. S., Allwardt, B., Gulcher, J. R., Mikol, D. D., Högnason, T., . . . Stefansson, K. (1998). Expression of the oligodendrocyte-myelin glycoprotein by neurons in the mouse central nervous system. *J Neurochem, 70*(4), 1704-1711. doi:10.1046/j.1471-4159.1998.70041704.x

He, R., Han, W., Song, X., Cheng, L., Chen, H., & Jiang, L. (2021). Knockdown of Lingo-1 by short hairpin RNA promotes cognitive function recovery in a status convulsion model. *3 Biotech, 11*(7), 339. doi:10.1007/s13205-021-02876-8

Hennes, E. M., Baumann, M., Schanda, K., Anlar, B., Bajer-Kornek, B., Blaschek, A., . . . Rostásy, K. (2017). Prognostic relevance of MOG antibodies in children with an

acquired demyelinating syndrome. *Neurology, 89*(9), 900-908. doi:10.1212/wnl.0000000000004312

Hor, J. Y., & Fujihara, K. (2023). Epidemiology of myelin oligodendrocyte glycoprotein antibody-associated disease: a review of prevalence and incidence worldwide. *Front Neurol, 14*, 1260358. doi:10.3389/fneur.2023.1260358

Hu, X., Wang, J. Y., Gu, R., Qu, H., Li, M., Chen, L., . . . Yuan, P. (2016). The relationship between the occurrence of intractable epilepsy with glial cells and myelin sheath - an experimental study. *Eur Rev Med Pharmacol Sci, 20*(21), 4516-4524.

Huang, J. K., Phillips, G. R., Roth, A. D., Pedraza, L., Shan, W., Belkaid, W., . . . Colman, D. R. (2005). Glial membranes at the node of Ranvier prevent neurite outgrowth. *Science, 310*(5755), 1813-1817. doi:10.1126/science.1118313

Jarius, S., Paul, F., Aktas, O., Asgari, N., Dale, R. C., de Seze, J., . . . Wildemann, B. (2018). MOG encephalomyelitis: international recommendations on diagnosis and antibody testing. *J Neuroinflammation, 15*(1), 134. doi:10.1186/s12974-018-1144-2

Jarius, S., & Wildemann, B. (2013). The history of neuromyelitis optica. *J Neuroinflammation, 10*, 8. doi:10.1186/1742-2094-10-8

Karlsson, T. E., Wellfelt, K., & Olson, L. (2017). Spatiotemporal and Long Lasting Modulation of 11 Key Nogo Signaling Genes in Response to Strong Neuroexcitation. *Front Mol Neurosci, 10*, 94. doi:10.3389/fnmol.2017.00094

Kitley, J., Woodhall, M., Waters, P., Leite, M. I., Devenney, E., Craig, J., . . . Vincent, A. (2012). Myelin-oligodendrocyte glycoprotein antibodies in adults with a neuromyelitis optica phenotype. *Neurology, 79*(12), 1273-1277. doi:10.1212/WNL.0b013e31826aac4e

Kottis, V., Thibault, P., Mikol, D., Xiao, Z. C., Zhang, R., Dergham, P., & Braun, P. E. (2002). Oligodendrocyte-myelin glycoprotein (OMgp) is an inhibitor of neurite outgrowth. *J Neurochem, 82*(6), 1566-1569. doi:10.1046/j.1471-4159.2002.01146.x

Krishnan, C., Kaplin, A. I., Pardo, C. A., Kerr, D. A., & Keswani, S. C. (2006). Demyelinating disorders: update on transverse myelitis. *Curr Neurol Neurosci Rep, 6*(3), 236-243. doi:10.1007/s11910-006-0011-1

Krupp, L. B., Tardieu, M., Amato, M. P., Banwell, B., Chitnis, T., Dale, R. C., . . . Wassmer, E. (2013). International Pediatric Multiple Sclerosis Study Group criteria for pediatric multiple sclerosis and immune-mediated central nervous system demyelinating disorders: revisions to the 2007 definitions. *Mult Scler, 19*(10), 1261-1267. doi:10.1177/1352458513484547

Laurén, J., Hu, F., Chin, J., Liao, J., Airaksinen, M. S., & Strittmatter, S. M. (2007). Characterization of myelin ligand complexes with neuronal Nogo-66 receptor family members. *J Biol Chem, 282*(8), 5715-5725. doi:10.1074/jbc.M609797200

Lee, J. K., Geoffroy, C. G., Chan, A. F., Tolentino, K. E., Crawford, M. J., Leal, M. A., . . . Zheng, B. (2010). Assessing spinal axon regeneration and sprouting in Nogo-, MAG-, and OMgp-deficient mice. *Neuron, 66*(5), 663-670. doi:10.1016/j.neuron.2010.05.002

Lee, X., Hu, Y., Zhang, Y., Yang, Z., Shao, Z., Qiu, M., . . . Mi, S. (2011). Oligodendrocyte differentiation and myelination defects in OMgp null mice. *Mol Cell Neurosci, 46*(4), 752-761. doi:10.1016/j.mcn.2011.02.008

Lennon, V. A., Wingerchuk, D. M., Kryzer, T. J., Pittock, S. J., Lucchinetti, C. F., Fujihara, K., . . . Weinshenker, B. G. (2004). A serum autoantibody marker of neuromyelitis optica: distinction from multiple sclerosis. *Lancet, 364*(9451), 2106-2112. doi:10.1016/s0140-6736(04)17551-x

Longbrake, E. (2022). Myelin Oligodendrocyte Glycoprotein-Associated Disorders. *Continuum (Minneap Minn), 28*(4), 1171-1193. doi:10.1212/con.0000000000001127

Love, S. (2006). Demyelinating diseases. *J Clin Pathol, 59*(11), 1151-1159. doi:10.1136/jcp.2005.031195

Mader, S., Kümpfel, T., & Meinl, E. (2020). Novel insights into pathophysiology and therapeutic possibilities reveal further differences between AQP4-IgG- and MOG-IgG-associated diseases. *Curr Opin Neurol, 33*(3), 362-371. doi:10.1097/wco.0000000000000813

Maglio, G., D'Agostino, M., Caronte, F. P., Pezone, L., Casamassimi, A., Rienzo, M., . . . Abbondanza, C. (2024). Multiple Sclerosis: From the Application of Oligoclonal Bands to Novel Potential Biomarkers. *Int J Mol Sci, 25*(10). doi:10.3390/ijms25105412

Martin, I., Andres, C. R., Védrine, S., Tabagh, R., Michelle, C., Jourdan, M. L., . . . Vourc'h, P. (2009). Effect of the oligodendrocyte myelin glycoprotein (OMgp) on the expansion and neuronal differentiation of rat neural stem cells. *Brain Res, 1284*, 22-30. doi:10.1016/j.brainres.2009.05.070

Massa, S., Fracchiolla, A., Neglia, C., Argentiero, A., & Esposito, S. (2021). Update on Acute Disseminated Encephalomyelitis in Children and Adolescents. *Children (Basel), 8*(4). doi:10.3390/children8040280

Matsumoto, Y., Misu, T., Mugikura, S., Takai, Y., Nishiyama, S., Kuroda, H., . . . Aoki, M. (2020). Distinctive lesions of brain MRI between MOG-antibody-associated and AQP4-antibody-associated diseases. *J Neurol Neurosurg Psychiatry*. doi:10.1136/jnnp-2020-324818

Miki, T., Yokoyama, T., Kusaka, T., Suzuki, S., Ohta, K., Warita, K., . . . Takeuchi, Y. (2014). Early postnatal repeated maternal deprivation causes a transient increase in OMpg and BDNF in rat cerebellum suggesting precocious myelination. *J Neurol Sci, 336*(1-2), 62-67. doi:10.1016/j.jns.2013.10.007

Mikol, D. D., Alexakos, M. J., Bayley, C. A., Lemons, R. S., Le Beau, M. M., & Stefansson, K. (1990). Structure and chromosomal localization of the gene for the oligodendrocyte-myelin glycoprotein. *J Cell Biol, 111*(6 Pt 1), 2673-2679. doi:10.1083/jcb.111.6.2673

Mikol, D. D., Gulcher, J. R., & Stefansson, K. (1990). The oligodendrocyte-myelin glycoprotein belongs to a distinct family of proteins and contains the HNK-1 carbohydrate. *J Cell Biol, 110*(2), 471-479. doi:10.1083/jcb.110.2.471

Mikol, D. D., & Stefansson, K. (1988). A phosphatidylinositol-linked peanut agglutinin-binding glycoprotein in central nervous system myelin and on oligodendrocytes. *J Cell Biol, 106*(4), 1273-1279. doi:10.1083/jcb.106.4.1273

Mironova, Y. A., & Giger, R. J. (2013). Where no synapses go: gatekeepers of circuit remodeling and synaptic strength. *Trends Neurosci, 36*(6), 363-373. doi:10.1016/j.tins.2013.04.003

Misu, T., Sato, D. K., Nakashima, I., & Fujihara, K. (2015). MOG-IgG serological status matters in paediatric ADEM. *Journal of Neurology, Neurosurgery & Psychiatry, 86*(3), 242-242. doi:10.1136/jnnp-2014-308723

Moheb, N., & Chen, J. J. (2023). The neuro-ophthalmological manifestations of NMOSD and MOGAD-a comprehensive review. *Eye (Lond), 37*(12), 2391-2398. doi:10.1038/s41433-023-02477-0

Neri, V. C., Xavier, M. F., Barros, P. O., Melo Bento, C., Marignier, R., & Papais Alvarenga, R. (2018). Case Report: Acute Transverse Myelitis after Zika Virus Infection. *Am J Trop Med Hyg, 99*(6), 1419-1421. doi:10.4269/ajtmh.17-0938

Nie, D. Y., Ma, Q. H., Law, J. W., Chia, C. P., Dhingra, N. K., Shimoda, Y., . . . Xiao, Z. C. (2006). Oligodendrocytes regulate formation of nodes of Ranvier via the recognition molecule OMgp. *Neuron Glia Biol, 2*(3), 151-164. doi:10.1017/s1740925x06000251

O'Connor, K. C., McLaughlin, K. A., De Jager, P. L., Chitnis, T., Bettelli, E., Xu, C., . . . Wucherpfennig, K. W. (2007). Self-antigen tetramers discriminate between myelin autoantibodies to native or denatured protein. *Nat Med, 13*(2), 211-217. doi:10.1038/nm1488

Paolilo, R. B., Deiva, K., Neuteboom, R., Rostásy, K., & Lim, M. (2020). Acute Disseminated Encephalomyelitis: Current Perspectives. *Children (Basel), 7*(11). doi:10.3390/children7110210

Pérez, C. A. (2021). Clinical Features of Multiple Sclerosis. In C. A. Perez, A. Smith, & F. Nelson (Eds.), *Multiple Sclerosis: A Practical Manual for Hospital and Outpatient Care* (pp. 21-36). Cambridge: Cambridge University Press.

Petzold, A., Fraser, C. L., Abegg, M., Alroughani, R., Alshowaeir, D., Alvarenga, R., . . . Plant, G. T. (2022). Diagnosis and classification of optic neuritis. *Lancet Neurol, 21*(12), 1120-1134. doi:10.1016/s1474-4422(22)00200-9

Preziosa, P., Amato, M. P., Battistini, L., Capobianco, M., Centonze, D., Cocco, E., . . . Filippi, M. (2024). Moving towards a new era for the treatment of neuromyelitis optica spectrum disorders. *J Neurol*. doi:10.1007/s00415-024-12426-w

Pröbstel, A. K., Dornmair, K., Bittner, R., Sperl, P., Jenne, D., Magalhaes, S., . . . Derfuss, T. (2011). Antibodies to MOG are transient in childhood acute disseminated encephalomyelitis. *Neurology, 77*(6), 580-588. doi:10.1212/WNL.0b013e318228c0b1

Promega. (2024). FuGENE® HD Transfection Reagent Technical Manual. Retrieved from https://worldwide.promega.com/resources/protocols/technical-manuals/101/fugene-hd-transfection-reagent-protocol/

Proposed diagnostic criteria and nosology of acute transverse myelitis. (2002). *Neurology, 59*(4), 499-505. doi:10.1212/wnl.59.4.499

Quagliata, M., Nuti, F., Real-Fernandez, F., Kirilova Kirilova, K., Santoro, F., Carotenuto, A., . . . Rovero, P. (2023). Glucopeptides derived from myelin-relevant proteins and hyperglucosylated nontypeable Haemophilus influenzae bacterial adhesin cross-react with multiple sclerosis specific antibodies: A step forward in the identification of native autoantigens in multiple sclerosis. *J Pept Sci, 29*(7), e3475. doi:10.1002/psc.3475

Raiker, S. J., Lee, H., Baldwin, K. T., Duan, Y., Shrager, P., & Giger, R. J. (2010). Oligodendrocyte-myelin glycoprotein and Nogo negatively regulate activity-dependent synaptic plasticity. *J Neurosci, 30*(37), 12432-12445. doi:10.1523/jneurosci.0895-10.2010

Reindl, M., Schanda, K., Woodhall, M., Tea, F., Ramanathan, S., Sagen, J., . . . Waters, P. (2020). International multicenter examination of MOG antibody assays. *Neurol Neuroimmunol Neuroinflamm, 7*(2). doi:10.1212/nxi.0000000000000674

Saha, N., Kolev, M., & Nikolov, D. B. (2014). Structural features of the Nogo receptor signaling complexes at the neuron/myelin interface. *Neurosci Res, 87*, 1-7. doi:10.1016/j.neures.2014.06.003

Santoro, J. D., & Chitnis, T. (2019). Diagnostic Considerations in Acute Disseminated Encephalomyelitis and the Interface with MOG Antibody. *Neuropediatrics, 50*(5), 273-279. doi:10.1055/s-0039-1693152

Sato, D. K., Callegaro, D., Lana-Peixoto, M. A., Waters, P. J., de Haidar Jorge, F. M., Takahashi, T., . . . Fujihara, K. (2014). Distinction between MOG antibody-positive and AQP4 antibody-positive NMO spectrum disorders. *Neurology, 82*(6), 474-481. doi:10.1212/wnl.0000000000000101

Simone CG, E. P. (2024). *Transverse Myelitis.* Retrieved from Available from: https://www.ncbi.nlm.nih.gov/books/NBK559302/

Siriratnam, P., Huda, S., Butzkueven, H., van der Walt, A., Jokubaitis, V., & Monif, M. (2023). A comprehensive review of the advances in neuromyelitis optica spectrum disorder. *Autoimmun Rev, 22*(12), 103465. doi:10.1016/j.autrev.2023.103465

Spadaro, M., & Meinl, E. (2016). Detection of Autoantibodies Against Myelin Oligodendrocyte Glycoprotein in Multiple Sclerosis and Related Diseases. *Methods Mol Biol, 1304*, 99-104. doi:10.1007/7651_2015_223

Spillers, N. J., Luther, P. M., Talbot, N. C., Kidder, E. J., Doyle, C. A., Lutfallah, S. C., . . . Varrassi, G. (2024). A Comparative Review of Typical and Atypical Optic Neuritis: Advancements in Treatments, Diagnostics, and Prognosis. *Cureus, 16*(3), e56094. doi:10.7759/cureus.56094

Stefan, K. A., & Ciotti, J. R. (2024). MOG Antibody Disease: Nuances in Presentation, Diagnosis, and Management. *Curr Neurol Neurosci Rep*. doi:10.1007/s11910-024-01344-z

Tea, F., Pilli, D., Ramanathan, S., Lopez, J. A., Merheb, V., Lee, F. X. Z., . . . Brilot, F. (2020). Effects of the Positive Threshold and Data Analysis on Human MOG Antibody Detection by Live Flow Cytometry. *Front Immunol, 11*, 119. doi:10.3389/fimmu.2020.00119

Toosy, A. T., Mason, D. F., & Miller, D. H. (2014). Optic neuritis. *Lancet Neurol, 13*(1), 83-99. doi:10.1016/s1474-4422(13)70259-x

Viskochil, D., Cawthon, R., O'Connell, P., Xu, G. F., Stevens, J., Culver, M., . . . White, R. (1991). The gene encoding the oligodendrocyte-myelin glycoprotein is embedded within the neurofibromatosis type 1 gene. *Mol Cell Biol, 11*(2), 906-912. doi:10.1128/mcb.11.2.906-912.1991

Vourc'h, P., & Andres, C. (2004). Oligodendrocyte myelin glycoprotein (OMgp): evolution, structure and function. *Brain Res Brain Res Rev, 45*(2), 115-124. doi:10.1016/j.brainresrev.2004.01.003

Vourc'h, P., Dessay, S., Mbarek, O., Marouillat Védrine, S., Müh, J. P., & Andres, C. (2003). The oligodendrocyte-myelin glycoprotein gene is highly expressed during the late stages of myelination in the rat central nervous system. *Brain Res Dev Brain Res, 144*(2), 159-168. doi:10.1016/s0165-3806(03)00167-6

Vourc'h, P., Moreau, T., Arbion, F., Marouillat-Védrine, S., Müh, J. P., & Andres, C. (2003). Oligodendrocyte myelin glycoprotein growth inhibition function requires its conserved leucine-rich repeat domain, not its glycosylphosphatidyl-inositol anchor. *J Neurochem, 85*(4), 889-897. doi:10.1046/j.1471-4159.2003.01764.x

Walton, C., King, R., Rechtman, L., Kaye, W., Leray, E., Marrie, R. A., . . . Baneke, P. (2020). Rising prevalence of multiple sclerosis worldwide: Insights from the Atlas of MS, third edition. *Multiple Sclerosis Journal, 26*(14), 1816-1821. doi:10.1177/1352458520970841

Wang, C. X. (2021). Assessment and Management of Acute Disseminated Encephalomyelitis (ADEM) in the Pediatric Patient. *Paediatr Drugs, 23*(3), 213-221. doi:10.1007/s40272-021-00441-7

Waters, P., Woodhall, M., O'Connor, K. C., Reindl, M., Lang, B., Sato, D. K., . . . Vincent, A. (2015). MOG cell-based assay detects non-MS patients with inflammatory neurologic disease. *Neurol Neuroimmunol Neuroinflamm, 2*(3), e89. doi:10.1212/nxi.0000000000000089

Waters, P. J., Komorowski, L., Woodhall, M., Lederer, S., Majed, M., Fryer, J., . . . Pittock, S. J. (2019). A multicenter comparison of MOG-IgG cell-based assays. *Neurology, 92*(11), e1250-e1255. doi:10.1212/wnl.0000000000007096

Waters, P. J., McKeon, A., Leite, M. I., Rajasekharan, S., Lennon, V. A., Villalobos, A., . . . Pittock, S. J. (2012). Serologic diagnosis of NMO: a multicenter comparison of aquaporin-4-IgG assays. *Neurology, 78*(9), 665-671; discussion 669. doi:10.1212/WNL.0b013e318248dec1

Waubant, E., Lucas, R., Mowry, E., Graves, J., Olsson, T., Alfredsson, L., & Langer-Gould, A. (2019). Environmental and genetic risk factors for MS: an integrated review. *Ann Clin Transl Neurol, 6*(9), 1905-1922. doi:10.1002/acn3.50862

Weinshenker, B. G., & Wingerchuk, D. M. (2017). Neuromyelitis Spectrum Disorders. *Mayo Clin Proc, 92*(4), 663-679. doi:10.1016/j.mayocp.2016.12.014

Wingerchuk, D. M., Hogancamp, W. F., O'Brien, P. C., & Weinshenker, B. G. (1999). The clinical course of neuromyelitis optica (Devic's syndrome). *Neurology, 53*(5), 1107-1114. doi:10.1212/wnl.53.5.1107

Wingerchuk, D. M., Lennon, V. A., Pittock, S. J., Lucchinetti, C. F., & Weinshenker, B. G. (2006). Revised diagnostic criteria for neuromyelitis optica. *Neurology, 66*(10), 1485-1489. doi:10.1212/01.wnl.0000216139.44259.74

Winklmeier, S., Schlüter, M., Spadaro, M., Thaler, F. S., Vural, A., Gerhards, R., . . . Meinl, E. (2019). Identification of circulating MOG-specific B cells in patients with MOG antibodies. *Neurol Neuroimmunol Neuroinflamm, 6*(6), 625. doi:10.1212/nxi.0000000000000625

Woo, M. S., Engler, J. B., & Friese, M. A. (2024). The neuropathobiology of multiple sclerosis. *Nat Rev Neurosci*. doi:10.1038/s41583-024-00823-z

Xu, C.-J., Wang, J.-L., & Jin, W.-L. (2015). The Neural Stem Cell Microenvironment: Focusing on Axon Guidance Molecules and Myelin-Associated Factors. *Journal of Molecular Neuroscience, 56*(4), 887-897. doi:10.1007/s12031-015-0538-1

Yeh, E. A., & Nakashima, I. (2019). Live-cell based assays are the gold standard for anti-MOG-Ab testing. *Neurology, 92*(11), 501-502. doi:10.1212/wnl.0000000000007077

Zhang, Y., Chen, K., Sloan, S. A., Bennett, M. L., Scholze, A. R., O'Keeffe, S., . . . Wu, J. Q. (2014). An RNA-sequencing transcriptome and splicing database of glia, neurons, and vascular cells of the cerebral cortex. *J Neurosci, 34*(36), 11929-11947. doi:10.1523/jneurosci.1860-14.2014

Appendix A: SUPPLEMENTARY FIGURES

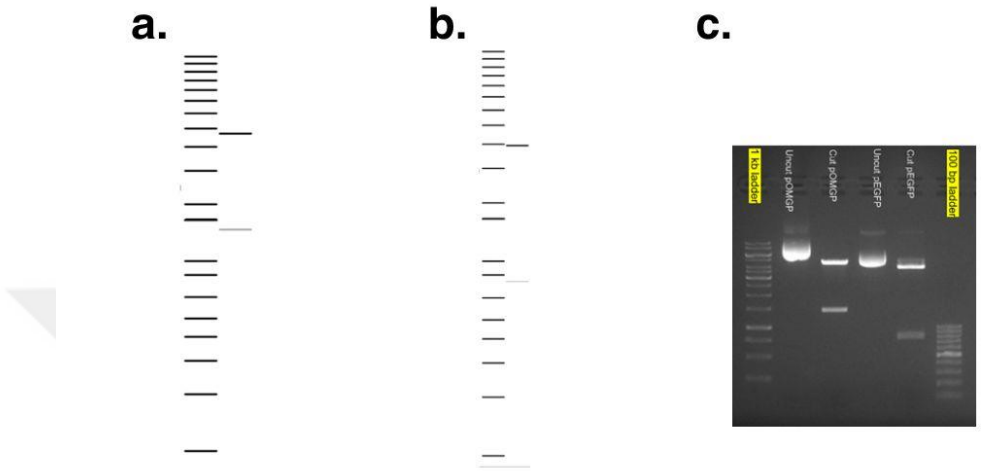

Appendix A Figure 1 : Visualization of diagnostic digestion outcomes with the Gel Doc XR+ Imaging System. While a) for the pOMGP-TM-GFP plasmid (upper band 4723 bp and lower band 1467 bp.) and b) for pEGFP-N1 plasmid (3964 bp upper 787 bp lower.) represent the bands expecting to see in agarose gel; c) The diagnostic digestion result in 1% agarose gel. Samples loaded on the gel, from left to right; 1kb ladder, uncut control pOMGP-TM-GFP plasmid, cut pOMGP-TM-GFP plasmid, uncut pEGFP-N1 plasmid, cut pEGFP-N1 plasmid, and 100 bp ladder.

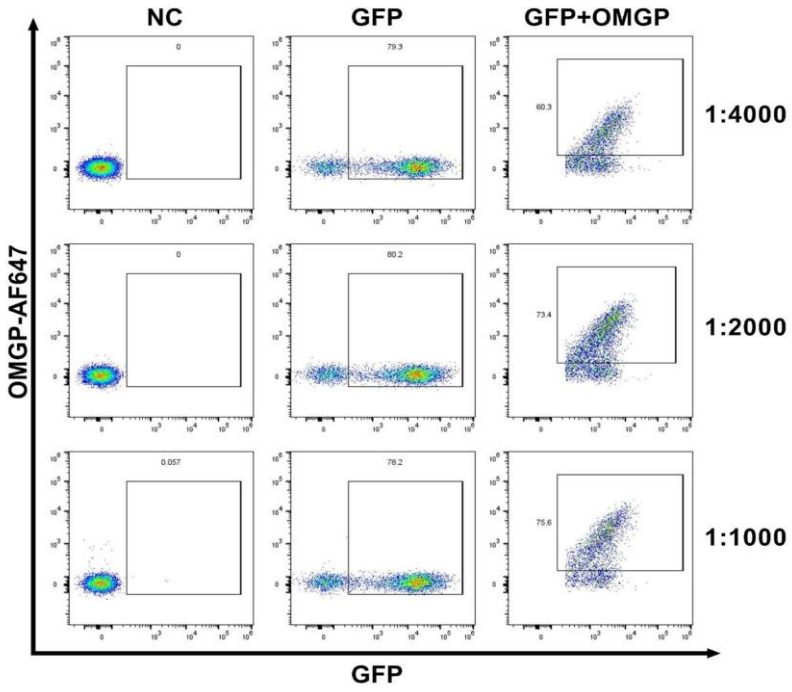

Appendix A Figure 2 : Optimization results of Alexa Fluor 647-conjugated Streptavidin antibody. NC group includes untransfected control group cells; GFP indicates pEGFP-N1 transfected cells, whereas GFP+ OMGP indicates pOMGP-TM-GFP transfected cells.

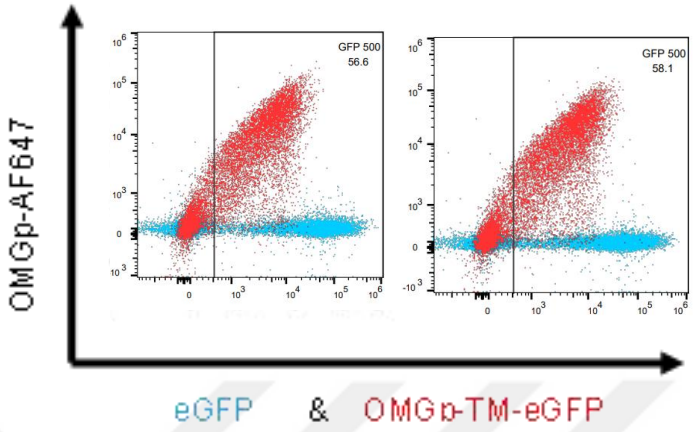

Appendix A Figure 3 : Measurement of 22H6 antibody tested at different dilution factors by flow cytometry. The one on the left shows a ratio of 1:100, and the one on the right shows a ratio of 1:200.

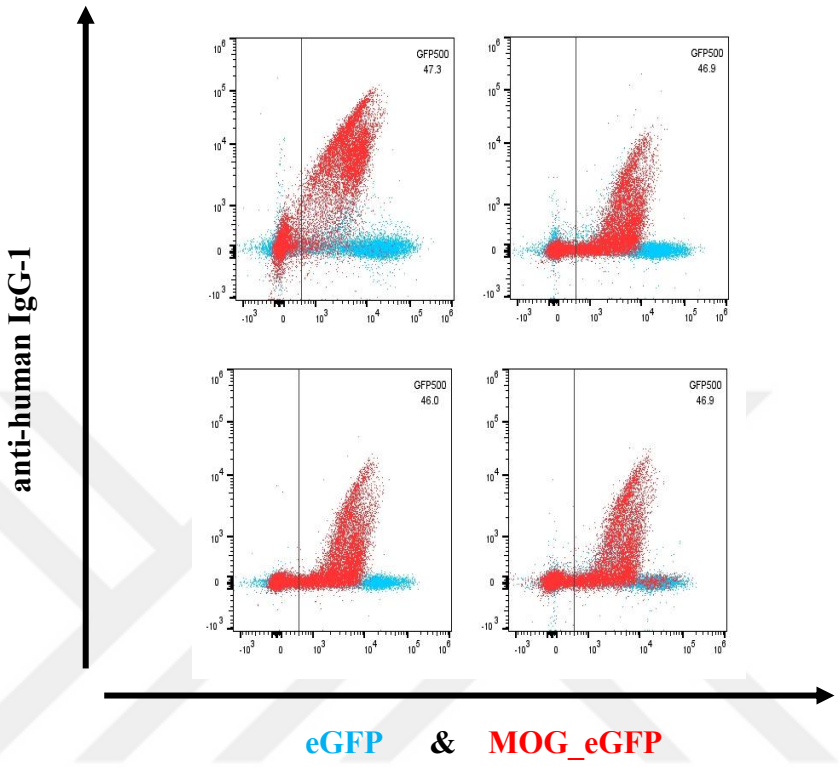

Appendix A Figure 4 The pilot study for IgG1 antibody. The live cell-based assay was carried out to investigate whether our antibody was functioning by using MOG-transfected cells and serum from patients known to be MOG-positive as a positive control.